The Tribological and Electrical Effects of Nanoparticle and Proprietary Lubricants

by

Larkin Crilly

A thesis submitted to the Graduate Faculty of
Auburn University
in partial fulfillment of the
requirements for the Degree of
Master of Science

Auburn, Alabama
May 1, 2021

Keywords: Nanolubricants, Wear, Electrical Contact Resistance, Contact Lubrication, Plated Contact, Silver Nanoparticles

Approved by

Robert L. Jackson, Chair, Professor of Mechanical Engineering
Kyle D. Schulze, Assistant Professor of Mechanical Engineering
George T. Flowers, Professor of Mechanical Engineering

Abstract

Electrical systems of any type rely upon electrical connectors or contacts; these may be found in places like computers, light switches, or electric vehicles and are present in a wide range of environments as a result. These contacts can often be subject to degradation from such things as fatigue and wear, particularly if they exist in machinery with a lot of vibrations; if this degradation makes the electrical contact resistance across the connector/contact change by too large an amount (how much depends on the application), the contact can fail or cause the system it is in to fail. As such, some contacts are lubricated to mitigate these effects. However, options are limited, as many lubricants and/or additives (e.g., ZDDP) are insulating or form insulating tribofilms. Nanoparticles have been the subject of much research in tribology for their unique properties, including friction reduction. More recently, some focus has been placed on their potential to be used in electrical contact applications. This thesis focuses on an investigation of the friction, wear, and electrical contact resistance properties at low loading (2N) of a dodecane-based silver nanoparticle lubricant as compared to a proprietary option, along with exploring the effects of adding the silver nanoparticles to this proprietary lubricant. Some discussion of the stability of these lubricants, particularly when adding particles to the proprietary lubricant, is undertaken along with an exploration of what lubrication regimes were present for the different lubricants.

Acknowledgments

I would like to thank my advisor, Dr. Robert Jackson, along with my committee members Dr. Kyle Schulze and Dr. George Flowers, for their guidance, expertise, and support in this endeavor. Additionally, many thanks to our Department of Chemistry and Biochemistry colleagues Mr. Samuel Bond and Dr. German Mills, as it was their preparation of silver nanoparticle colloids which allowed this investigation to take place. Thanks also to Dr. Greg Pawlikowski, Dr. Rod Martens, and Dr. Suvrat Bhargava of TE Connectivity for enabling this project and providing their support, expertise, and analysis. Furthermore, I thank our undergraduate research assistant, Ms. Emily Dickey, who helped run some of these tests.

I also would like to thank my parents and family, whose continuing support allowed this to be possible, along with my friends, whose support, humor, and (virtual) company helped keep me going at times during this past pandemic year.

In remembrance of my late aunt, Mona, who loved to travel, and who sadly left us this February. May her final journey be peaceful.

Table of Contents

List of Tables

List of Figures

List of Abbreviations

AWG	American Wire Gage
COF	Coefficient of Friction
DMM	Digital Multimeter
ECR	Electrical Contact Resistance
EDS	Energy-Dispersive X-Ray Spectroscopy
EHL	Elastohydrodynamic Lubrication
EV	Electric Vehicle
PLC	Power Line Cycles
RPM	Revolutions Per Minute
SEM	Scanning Electron Microscopy
ZDDP	Zinc-Diakyldithiophosphate

Chapter 1: Review and Introduction

Nearly all electrical systems depend on electrical contacts and connectors having a stable level of electrical contact resistance (ECR) across them. These connectors, like all material contact surfaces, feature microscopic roughness with peaks ('asperities') forcing imperfect contact between the surfaces. Materials only come into contact at these asperity peaks, reducing the contact area and, as conduction occurs through the asperity contacts (the gaps between them being filled with insulating materials like air), causing contact resistance between the surfaces (Fig. 1.1). The surface asperity configuration can be modified and worn down, however, leading to changes in the area of contact and, thus, changes to the contact resistance; if this change is great enough, the connector can be considered to have failed. The exact level of change required for failure varies based on application. The causes of these surface modifications can be numerous and depend on the environment the connector is in; connectors can be found in situations running the gamut from climate controlled (e.g., a home PC, televisions, etc.) to much harsher environments (e.g., inside a car or train, exposed to a corrosive atmosphere, etc.). In applications with severe vibrations, like inside a car engine, repeated micro sliding can occur and lead to fretting corrosion and/or wear and cause contact failure over time.

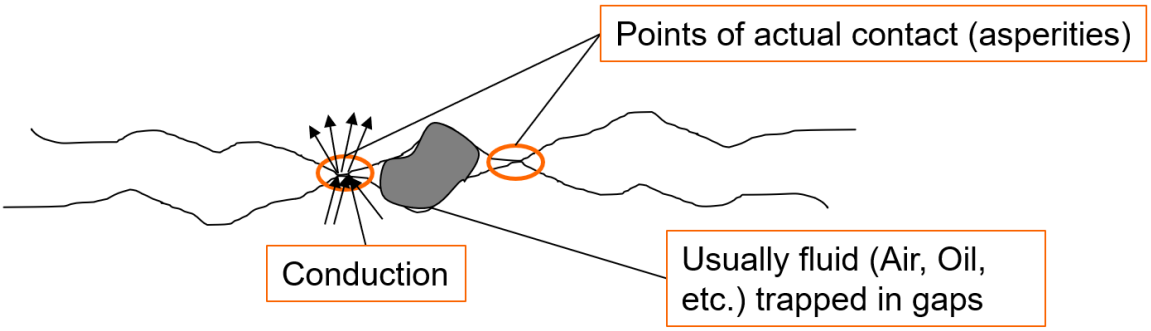

Figure 1.1: Diagram of typical contact

Lubricants have often been used to help prevent deterioration of electrical contacts. However, many lubricants and/or additives are insulating, resulting in large changes to ECR, and are therefore unsuited for electrical use. An example would be Zinc-Dialkyldithiophosphate (ZDDP), which forms an insulating tribofilm on surfaces (Fig. 1.2) [1, 2]. Thus, it is desirable to find alternative methods which can reduce wear without insulating the surface.

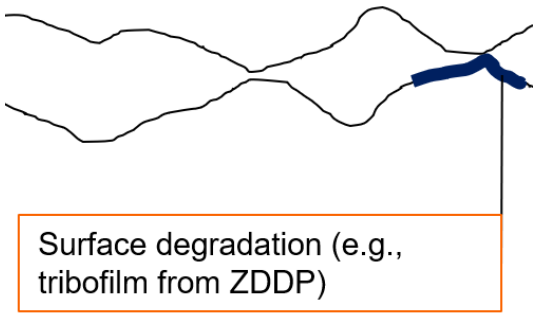

Figure 1.2: Diagram of Contact Degradation

Nanoparticles have various unique properties (e.g., they are usually harder than their bulk material counterparts [3, 4]) which have made them the subject of much research over the years. This largely started with research into the enhancement of fluid thermal conductivity and other thermal property enhancements [5-7] and has continued into explorations of their tribological effects.

It has been well documented that nanoparticles suspended within liquid lubricants can affect both friction and wear [8-19], usually in direct correlation with particle concentration levels [8-10, 17]. This has made them a subject of continual research, resulting in several mechanisms having been proposed to explain these improvements, including: the reduction of real contact area [20], surface polishing [14, 19], mending and/or surface modification [13, 19], having the particles act as nano-ball bearings [10-12,

16], film deposition [11, 12], or a combination of these and/or other factors [11, 12, 16]. However, there is no universally agreed upon mechanism(s) for friction improvements at this time.

Recently, some exploration of silver nanoparticles showed potential for benefits when used within electrical contacts [2]. While numerous particle materials have been studied, metallic particles have potential to both reduce wear, with the associated ECR changes that can result, and also potentially increase the conductivity of a lubricant [21]. In one prior paper, it was found that adding a single drop of a copper nanoparticle-laden lubricant during a test reduced the ECR immediately after application [18]. These early explorations used loads higher than many contact applications would face (contact loads are rarely above ~10N [22]), however, along with using materials not as common in electrical connectors.

The research for this thesis explores the friction, wear, and ECR effects of nanoparticles in further depth using multiple silver nanoparticle-enhanced lubricants as compared to their base oil and a proprietary lubricant. Additionally, the effects of adding these silver nanoparticles to the proprietary lubricant were explored. This work was conducted with actual electrical contact samples (provided by our partners at TE Connectivity) plated with either silver or gold, with tests run at a lighter contact load (2N) than in these prior works. Multiple variable-speed tests were run to generate Stribeck curves of the studied lubricants and gain insight into the lubrication regimes present, along with continuous speed tests of selected lubricants. Additionally, the friction levels and wear scar widths were compared. The changes in ECR across tests were measured and compared. Selected sample sets were sent for SEM/EDS analysis at TE Connectivity, with

selected results from the SEM/EDS regarding the wear morphology of the tests being compared and discussed.

Though electric vehicle (EV) motor bearings were not the focus of this research, certain results regarding the friction characteristics of the dodecane nanolubricants indicate they might have some benefit. Specifically, EVs tend to use lower viscosity lubricants and are thus faced with higher initial friction [23]; this is briefly discussed further in Ch. 3 as the dodecane nanolubricants exhibited lower friction at lower speeds on silver samples. EVs also face electrical wear in their motor bearings due to induced shaft voltages causing electrical discharge machining [24, 25]; though there are existing methods to deal with this, conductive lubricants have also been investigated and have shown some promise as a control method [26]. Since there is some evidence that particles can be used to directly increase the conductivity of lubricants [21], they are a potential option for such situations if a low-wear colloid could be found.

One of the tested lubricants was a version of the proprietary lubricant with the silver nanoparticles added. This ‘proprietary colloid’ featured numerous stability issues, which are detailed (along with stability comparisons to the dodecane nanolubricant) in Ch. 6. While there were no definitive signs that a full-film lubrication condition was reached during the Stribeck tests (the inbuilt Bruker ECR readout, see Ch. 2, did not indicate surface separation), some calculations of the film thickness for the dodecane were performed and are detailed in Ch. 7.

Chapter 2: Experimental Methods

The primary tests of interest for this research were Stribeck/wear tests to explore the lubrication regimes (Ch. 3), with ECR measurements being taken at appropriate times (Ch. 4). Select samples were later sent for SEM/EDS analysis (Ch. 5) and secondary observations of lubricant stability (Ch. 6) were performed along the way. Additionally, estimates of the hydrodynamic film thickness for dodecane were calculated (Ch. 7).

For all friction/wear test cases, the test setup consisted of a Bruker UMT-3 tester configured for a 'pin-on-disk' test, as seen in Fig. 2.1. Custom aluminum fixtures were devised to allow the use of electrical contact samples in these tests. These samples (Fig. 2.2) were provided by TE Connectivity and consisted of 1.20 cm x 2.54 cm x 0.04 cm rectangular plates (the 'disk', as measured with calipers) and ~7 mm diameter hemispherical caps (the 'pin') with a radius of curvature of ~3.43 mm as calculated from white light interferometer measurements of a non-plated bronze sample (Fig. 2.2, also see Fig. 7.1 in Ch. 7). Each plated sample was made of a phosphor bronze core plated with a nickel barrier layer, along with an additional 1.52 μm silver or 1.02 μm gold plating over top of the nickel. The silver samples were entirely plated, while the gold samples were only plated on one side (Fig. 2.3). The nominal average surface roughness values for silver samples (R_a) were 0.95-1.07 μm, while the gold samples were 0.34-0.35 μm, as provided by TE.

The plate samples were held within the aluminum fixture via parallel 'pinning' bars secured by four 18-8 stainless steel #3-48x1/2" socket head cap screws (Fig. 2.1). During sample plate mounting, these bolts were slowly tightened by moving to opposite corners and turning each screw approximately ¼ turn each time to help keep even pressure and a

level plate surface. These sample plates had a very slight curvature; as such, each sample was inserted with the curvature upward so that the 'pinning' bars could help flatten the surface (Fig. 2.4).

Additional 'framing' material kept the samples together during storage and shipping (can be seen in Fig. 2.2); this material had to be removed from each sample set before tests. Each sample was cut out of the framing material using scissors, leaving small burrs and rough edges. 240 grit sandpaper was used to carefully remove these burrs and smooth the edges of the samples without damaging the surface region being tested. This ensured that the samples would sit properly and consistently within the custom fixtures.

Each cap was held on a custom rod with a hand-tightened #7/16-20 threaded compression ring during tests. Additionally, both fixtures featured attachment points for electrical wiring to facilitate electrical contact resistance (ECR) measurements (Fig. 2.1). The rod, in particular, had the wiring connected at all times after initial attachment. All tests were set to create a ~2.6 mm radius wear scar in the flat plate.

The Bruker UMT-3 was additionally set up to measure ECR ('Bruker ECR') during tests via an inbuilt module connected to the bottom of the lower drive assembly (Fig. 2.5) and the compression fixture for the pin holder (Fig. 2.1 & 2.5). The data collected via this method was lower resolution and served mainly as an indicator of when the pin and disk were in contact during tests. To collect data for all later comparisons, a higher resolution external Agilent 34410A digital multimeter (DMM) connected to a PC was used. This DMM was set up for a 4-wire resistance measurement. ECR data was collected at the following three times during tests: a) before lubricant application, b) immediately before a test (with lubricant on the plate), and c) immediately after a test (while lubricant was still

on the plate). The custom pin and plate fixtures were connected to the DMM via 14 AWG multistrand wire with crimped ring terminals. These terminals were fastened to the electrical connection points with #8-32x1/4" socket head cap screws. Being a fixed connection, the wires for the plate holding fixture (the moving portion) had to be removed during test operations. It was found that the ECR measurement was repeatable across such disconnect/reconnect operations.

Each typical ECR measurement collected by the computer consisted of 30 samples taken over a ~1.5-minute period with an integration time of "100 PLC" to provide a resolution of 3.0e-5 Ohms. This was repeated at least four times at each stage of ECR collection to help smooth out any noise or transient effects. Between each ECR collection period, the pin was raised just out of contact with the surface as indicated via the Bruker ECR readout. Some late experiments would instead measure 120 samples at once over a ~6.5-minute period, occasionally being repeated in the case of transient effects, without moving the pin out of contact between each set of 30 samples (to attempt noise reduction). The measurement data (90 sequential samples relatively noise-free) was then averaged before and after the test and used to find the change in ECR resulting from each test (more details in Ch. 4).

Additional equipment used for measurements included a Veeco Dektak 150 Stylus Profilometer for roughness and wear scar measurement attempts, an AND HR200 scale for obtaining the mass of the samples, and a Bausch & Lomb StereoZoom7 optical microscope (up to 7x magnification) with a calibration slide for obtaining the approximate width of the wear scars. Plastic culture dishes were used to hold samples coated with the TE provided ('proprietary') lubricant and the derivative proprietary colloids ('proprietary colloid' and

‘proprietary solvent colloid’) made with it during the 24-hour drying process (discussed later this chapter). A Hitachi SU 6600 VPSEM with an Oxford EDS detector was used for SEM/EDS analysis on select samples sent to TE Connectivity. A 20 kV accelerating voltage with a working distance of 10-15 mm was used for these.

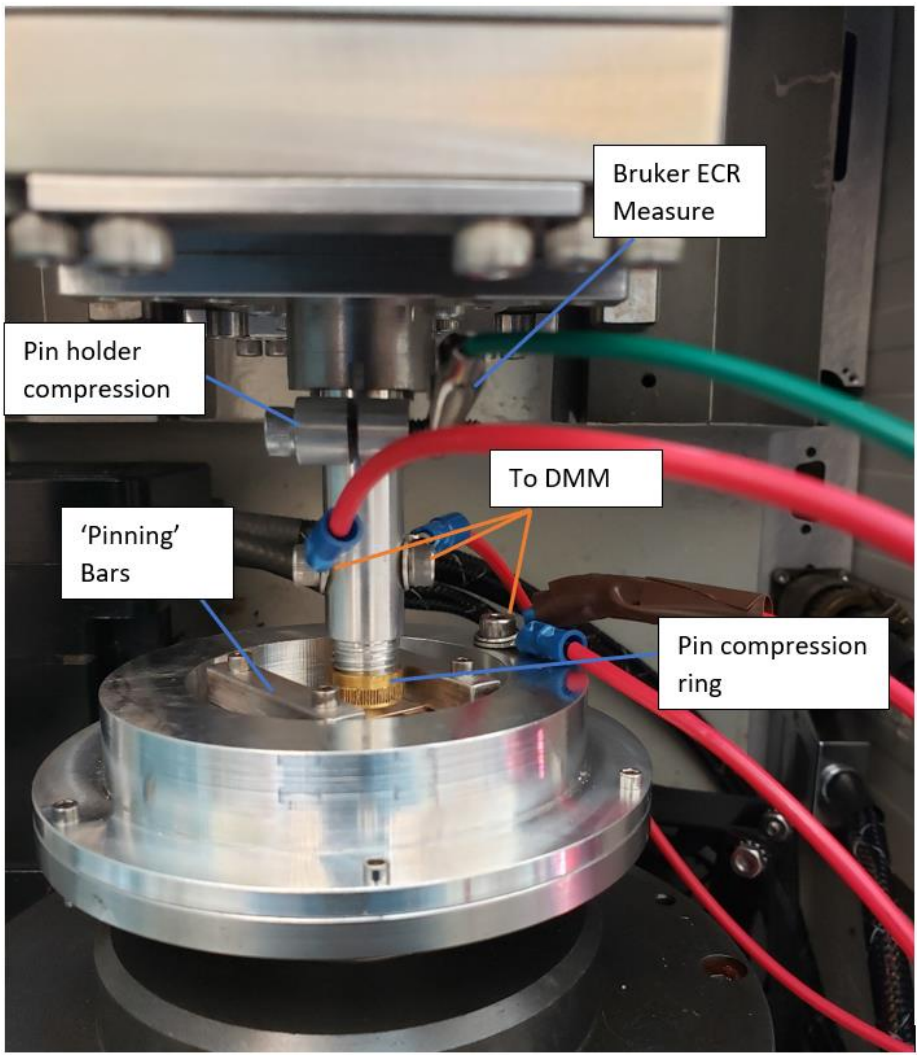

Figure 2.1: Fixtures in the Bruker

A new sample set was used for each test and all samples were cleaned prior to tests to ensure consistent surface quality. Cleaning of samples and equipment followed a common procedure:

- Apply acetone to the object to be cleaned, then wipe down with lint free wipe(s)
- Apply methanol to the object to be cleaned, then wipe down with lint free wipe(s)

With the surface being allowed to dry between the acetone and methanol applications. The only objects which did not fully receive this treatment were the culture dishes, as the plastic would melt from acetone exposure. Here, methanol and lint free wipes were exclusively used. Also, the threaded holes for the pinning bars (Fig. 2.6) were dried with rolled lint free wipes after the main exterior surfaces had been dried to prevent contamination of samples from residual acetone or methanol caught in the holes. All plates and caps were cleaned immediately before the collection of the first set of ECR data (the one before lubricant application) and after the final collection of ECR (or, if applicable, microscope images) at the end of tests. Lint free wipes were used to remove excess lubricant from the sample surfaces at this stage before applying acetone to reduce the chance of additional precipitation and/or deposition of the particles; the samples were also immediately wiped once acetone was applied for the same reason. Additionally, the samples were weighed before and after each test to see if a significant amount of mass was lost via wear.

Lubricant application was handled in the same manner for nearly all tests, as detailed in this chapter. All dodecane-based tests had 0.25 mL of lubricant applied to the plate via pipette while mounted in the Bruker immediately prior to bringing the cap into contact with the plate. The cap would then be raised no more than 2 mm (<1 mm in most

experiments) above the plate surface until after the experiment was complete to ensure that the meniscus (Fig. 2.7) did not collapse. As detailed in Ch. 3, it is possible that meniscus collapses resulted in some observed outlying data.

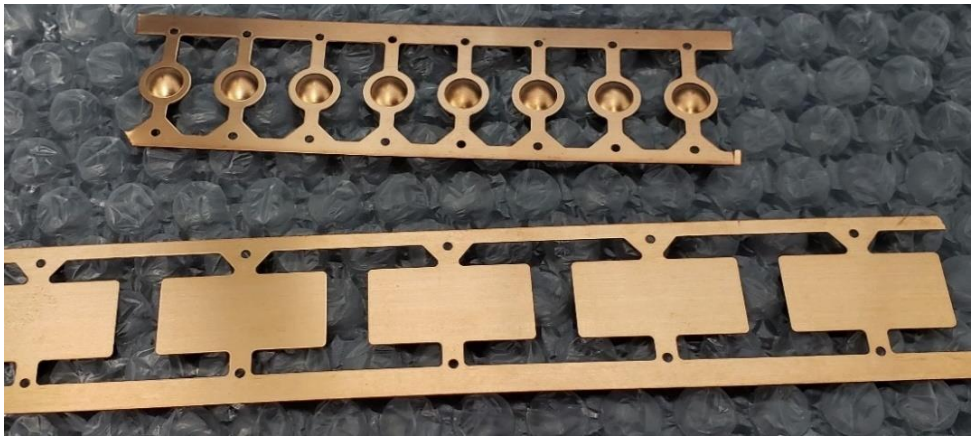

Figure 2.2: Unplated Samples

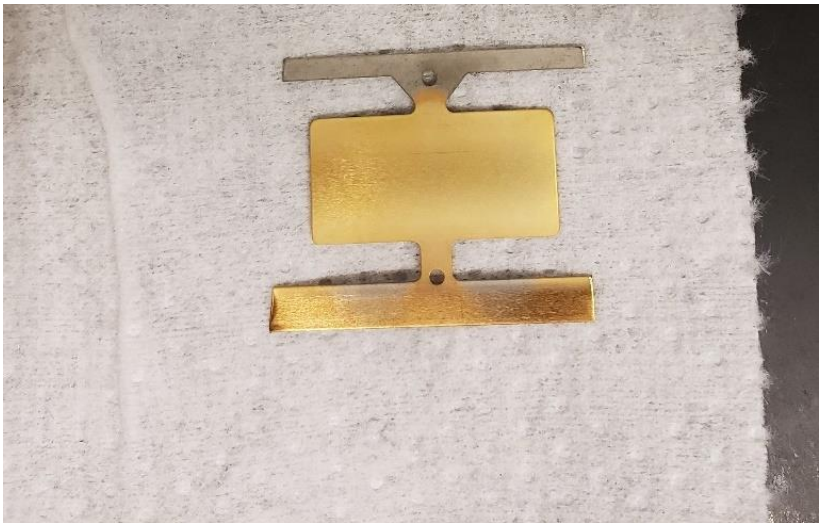

Figure 2.3: Plate sample with gold plated on one side

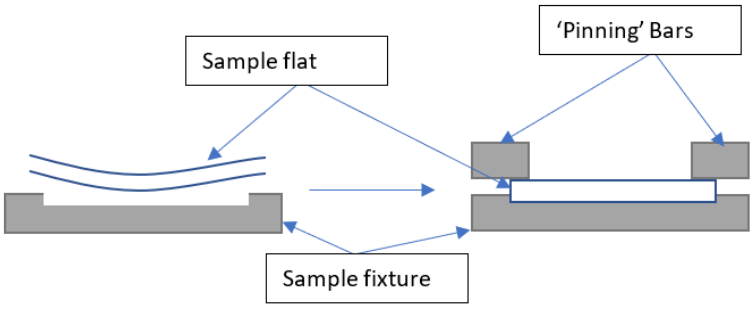

Figure 2.4: Diagram of sample plate curvature

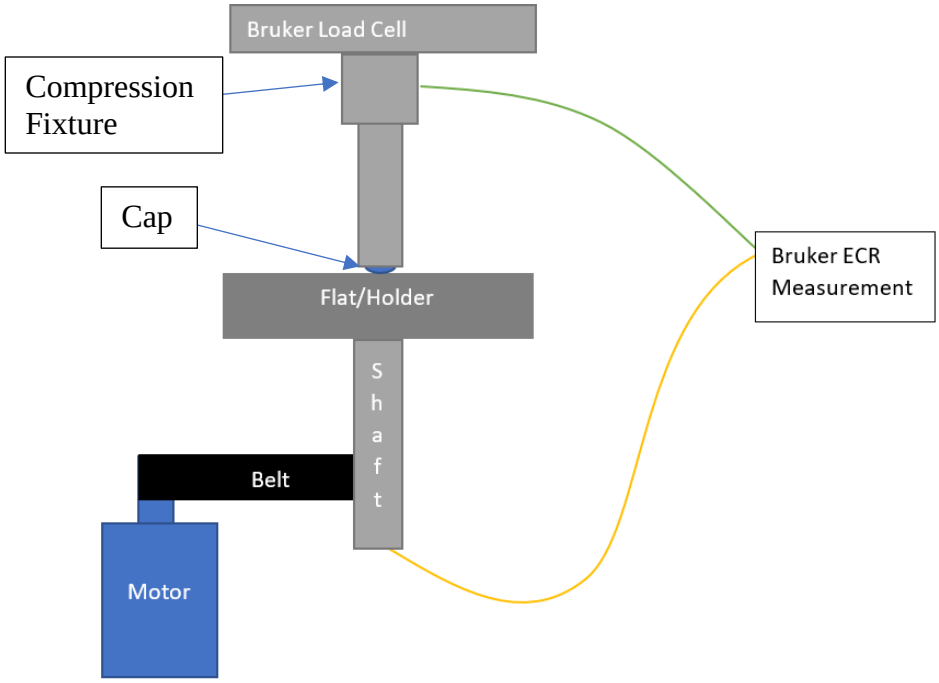

Figure 2.5: Diagram of Bruker

For tests involving the proprietary lubricant, whether it was unmodified or having had silver nanoparticles added via the proprietary solvent colloid (to get 'proprietary colloid'), or its components (when testing the 'proprietary solvent colloid' alone), 0.25 mL (for proprietary lubricant and proprietary solvent colloid) or 0.5 mL (for proprietary colloid) was applied via pipette to the sample plate after it had been relocated to a culture dish under a vent (to remove vapor). This was done because the proprietary lubricant was suspended within a solvent designed to evaporate during a drying period, leaving grease-like film on the surface. Application was done after collecting the ECR data from the dry sample set. The sample was then immediately covered with the dish lid and left to dry for 24 hours before carefully remounting the coated plate in the fixture and performing the desired test routine. For tests using a mixture of the nanoparticle solvent and lubricant, the 0.5 mL (0.25 mL from each of the mixture components) was mixed immediately prior to

application to the plate to prevent precipitation during storage (this instability is discussed more later this chapter and in Ch. 6).

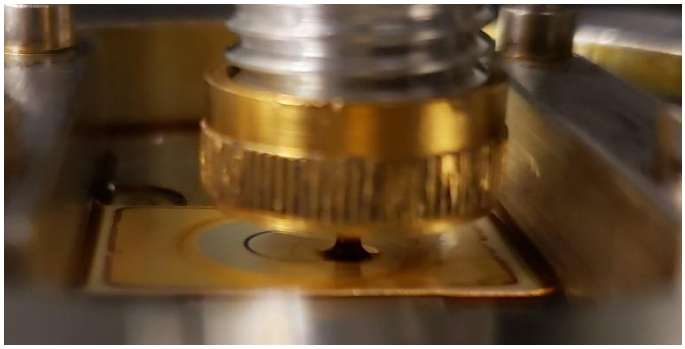

Figure 2.6: Dodecane nanolubricant meniscus

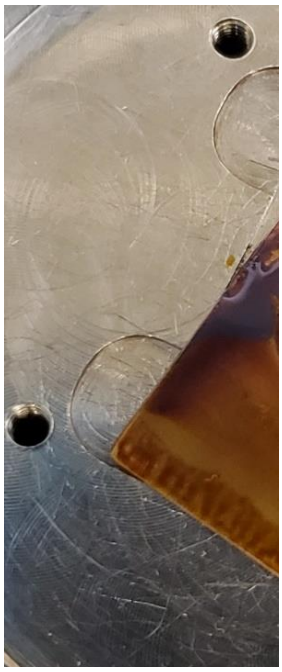

Figure 2.7: Mounting holes in plate fixture

Nanolubricant synthesis

Synthesis of the silver nanoparticles, whether within dodecane or the proprietary solvent, was performed by our colleagues in the Department of Chemistry and Biochemistry. The process involved the fast reduction of silver ions (as provided by silver neodecanoate) within the dodecane base oil at ~180 ^{o}C using oleyl sarcosine as a surfactant/stabilizer [6]. A transmission electron microscopy (TEM) image of the particles within dodecane (1.3 wt% or 0.1 M) is included in Fig. 2.8; these particles had an average diameter of ~5 nm [6]. The dodecane colloids, as synthesized, were stable for months under cool/dry/dark conditions. However, stability issues were found when combining the proprietary solvent colloid with the proprietary lubricant (to make the proprietary colloid):

precipitation would occur soon after mixing, possibly because of the dilution of the oleyl sarcosine affecting stability (although this was not present in the even more dilute dodecane colloids). An example of this precipitation is included in Fig. 2.9. Additionally, after several months, the proprietary solvent colloid itself began to show possible signs of separation (Fig. 2.10). All nanolubricants were stored in glass containers, with the proprietary lubricant stored in its TE-provided plastic container, at room temperature.

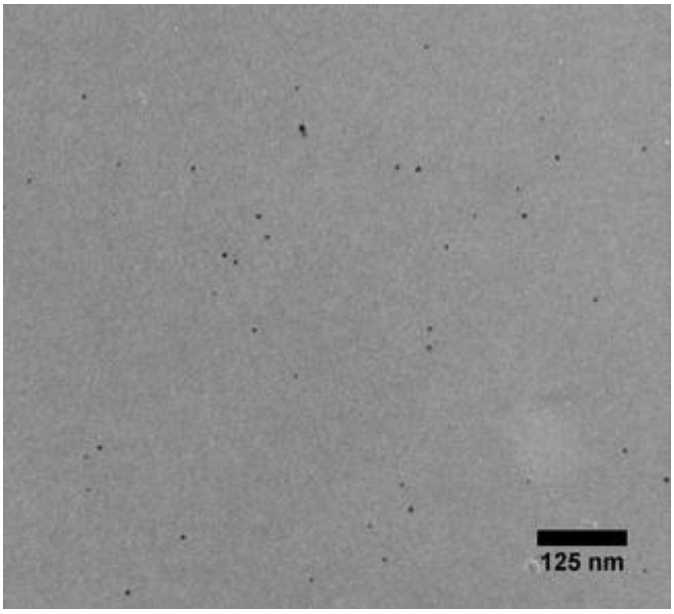

Figure 2.8: TEM image of silver particles within dodecane [6]

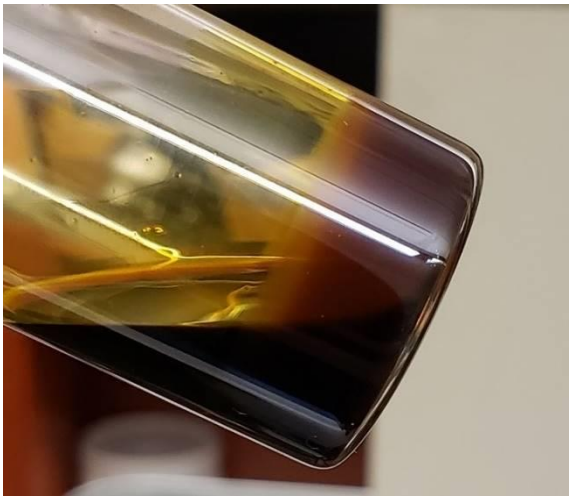

Figure 2.9: Proprietary colloid precipitation

Figure 2.10: Proprietary solvent colloid 'separation' (inside white circle)

Nanolubricant Dilution Creation

Several dilutions of the dodecane nanolubricant (full particle concentration of 1.3 wt%) were created to explore the effects of particle concentration on wear, friction, and ECR: 0.65 wt%, 0.325 wt%, and 0.163 wt% particle concentrations. These were created by adding an appropriate amount of pure dodecane base oil to the nanolubricant by mass as measured with the scale (Fig 2.11) and mixing them. These dilutions have proven to be as stable as the full concentration under the same cool/dry/dark conditions.

Figure 2.11: Nanolubricant dilution in progress

For the proprietary lubricant, particles were introduced via a modified version of the solvent containing silver nanoparticles (‘proprietary solvent colloid’). This was done by mixing equal volumes of the proprietary lubricant with the proprietary solvent colloid (initial concentration ~1.3 wt%) and mixing them (yielding ‘proprietary colloid’). This was done immediately prior to application for most tests due to the aforementioned issues with

colloid stability. This instability seems to manifest in some ways even under these conditions, however, as the surface of the resulting ‘film’ on the plate was usually not smooth after drying (Fig. 2.12; further discussed in Ch. 6).

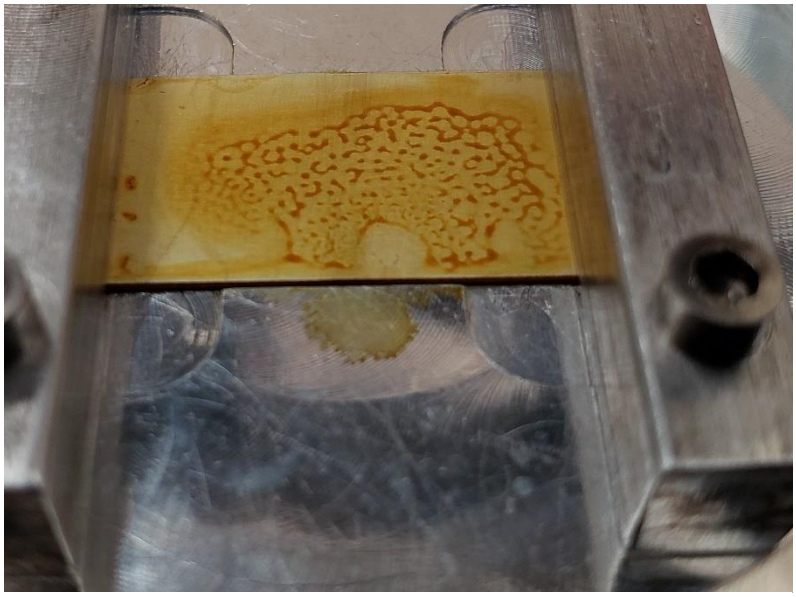

Figure 2.12: Example of nonuniform surface from proprietary nanolubricant colloid

Stribeck Test Procedure

Stribeck tests were the primary tests used to characterize the lubricant friction, wear, and ECR effects. The data from these varying speed tests were used to create Stribeck curves for each lubricant type and gain insight into the lubrication regimes present. A constant 2 N normal load (among the typical loads found for electrical contacts [22]) was applied while the bottom plate was rotated at varying speeds starting at 600 rpm and decreasing (see table 2.1), holding each at speed for three minutes.

Table 2.1: Speeds and timing for Stribeck tests

Speeds (rpm)	Linear Speed (m/s)	Timing
600, 500, 400, 300, 250, 200, 150, 100, 50, 25, 10, 5	0.163, 0.136, 0.109, 0.082, 0.068, 0.054, 0.041, 0.027, 0.014, 0.007, 0.003, 0.001	3 minutes at each speed

Constant Speed Test Procedure

As will be detailed further in Ch. 3, the data from the dodecane nanolubricant Stribeck tests using silver samples showed unusual friction decreases at low speeds. To help clarify what caused these results, additional tests were performed at constant speeds of either 10 RPM or 25 RPM. These used the same 2 N normal loading as the Stribeck tests, primarily using 1.3 wt% dodecane nanolubricant. It was calculated that, during the Stribeck tests, the sample makes 7770 complete rotations; to ensure that the same distance was covered by the constant speed tests, a 777-minute runtime was used for 10 RPM and a 310.8-minute runtime for 25 RPM.

Brief Lubricant Stability Note

In addition to the previously mentioned stability observations, some sample plates were left in covered culture dishes for extended periods with either the proprietary or dodecane nanolubricants left on the surface. Observations of the film changes over time were made via optical microscope. Full details of these observations are in Ch. 6.

Chapter 3–Results: Friction and Wear

One of the goals of this research was to obtain information about the friction regime behavior of the lubricants. This was accomplished by running tests at varying speeds to generate Stribeck curves for comparison. A typical Stribeck curve may be seen in Fig. 3.1. Here, the friction force is on the y-axis while speed is on the x-axis. For the purposes of this research, as the proprietary lubricant leaves a grease-like film without a known viscosity on the surface, friction plots were created using the Coefficient of Friction (COF) on the y-axis, and rotational speed in RPM on the x-axis.

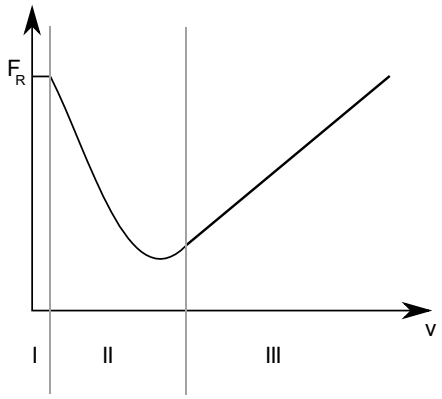

Figure 3.1: General Stribeck curve [27]

The three typical friction regimes found with lubricants can be seen on the Stribeck curve in Fig. 3.1:

- Regime I, or Boundary Lubrication, where the friction is highest as the contact area between surfaces is highest; most traditional lubricants reduce friction here by reducing surface adhesion via chemical effects.
- Regime II, or Mixed Lubrication, where there is still significant contact between the surface asperities although fluid pressure/film begins to separate them and

reduce friction, possibly including Elasto-hydrodynamic Lubrication (EHL) effects.

- Regime III, or Full Film/Hydrodynamic Lubrication, where the surfaces are completely separated by a film of lubricant sustained by the high fluid pressures generated from the high speed. Note that friction levels are typically at their lowest in this regime, with increases in friction resuming as the fluid film thickness grows and fluid shearing/viscosity begin to make an impact.

Generally, electrical contacts should stay in the Boundary regime, as reducing contact would result in potentially unacceptable levels of ECR change. A calculation of the dodecane film thickness (Ch. 7) at the highest speed tested showed that the boundary regime was likely not exceeded.

For each lubricant, a minimum of three Stribeck tests were performed, with each test varying speed according to Table 2.1 in Ch. 2. To attempt to minimize the effects of accumulated wear on the friction values, speeds were started at the high end, where hydrodynamic effects potentially reduce solid contact between the surfaces, then decreased.

At each speed within a given Stribeck test, the average COF was calculated and recorded. Another average was taken of these across the three (or more, if applicable) Stribeck tests to form the average Stribeck curve used for comparisons between lubricants. For each of these overall curves, the standard error was calculated and plotted based on these recorded average COF values over at least three individual tests.

Limited additional tests were conducted at constant speeds of either 10 RPM (0.003 m/s) or 25 RPM (0.007 m/s) using either the 1.3 wt% dodecane nanolubricant or the

proprietary lubricant with the silver samples. These tests were conducted to clarify the causes of the observed drops in friction at low speeds in the nanolubricant silver sample Stribeck tests (discussed further later this chapter). Note that, according to the typical Stribeck curve (Fig. 3.1), the friction should be higher at low speeds.

Attempts were made to characterize the wear scars using a Veeco Dektak 150 stylus profilometer and measuring the change in sample mass from experiments. However, in most cases, the scars were not discernable from these methods. As such, the primary method used to characterize the wear for comparisons was to measure the scar width via an optical microscope and calibration slide (see Fig. 3.2 for an example). Selected samples were also sent for SEM/EDS analysis (Ch. 5). As with the Stribeck curves, the standard error was calculated and plotted as error bars on the average scar width plots.

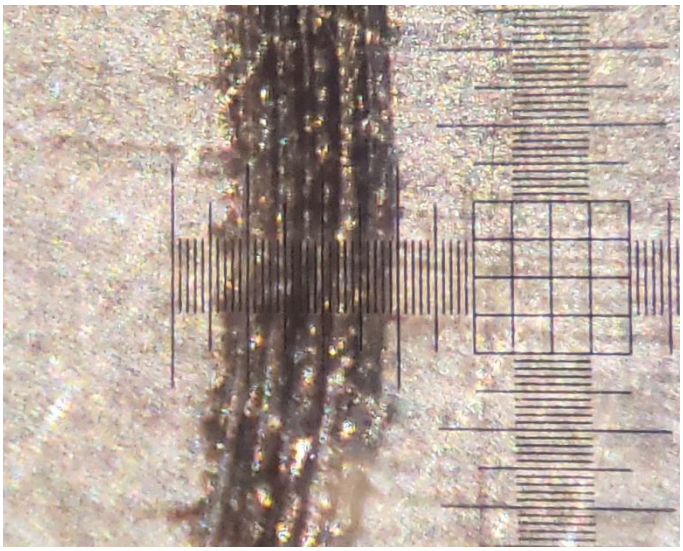

Figure 3.2: Example of wear scar width measurement

What follows in this chapter is an overview of the various unmodified lubricants followed by an overview of the nanolubricants and a comparison/discussion of the friction and wear results.

Individual Test Stribeck Curves

Outliers in the nanolubricant dilutions (discussed later this chapter) notwithstanding, the pure dodecane (0 wt%) on silver sample tests featured the highest COF values along with the largest COF spread (see Fig. 3.3). As might be expected, the wear scar widths also varied significantly in these tests, indicating that, under these severe wear conditions, there were probably competing wear mechanisms present. However, the SEM and EDS analyses performed on the 0 wt% samples indicate that adhesion was the dominant wear mechanism (Ch. 5). It should be noted that the curves do not strictly resemble that of a typical Stribeck curve with defined boundary (I), mixed/EHL (II), and full-film (III) regimes (see Fig. 3.1) and are instead rather flat [27]. This indicates that these tests likely never left the boundary lubrication regime, or at most, only started to enter EHL.

On average, the proprietary lubricant on silver samples had the lowest COF values and relatively low variance between tests. Of the various lubricants tested, the proprietary lubricant resulted in the most typical-looking Stribeck curves (Fig. 3.4). Considering the grease-like nature of the proprietary lubricant as compared to dodecane, it appeared that the EHL or full-film regime was possibly reached; though, as the Bruker ECR measurements did not indicate full surface separation, the full-film regime is less likely.

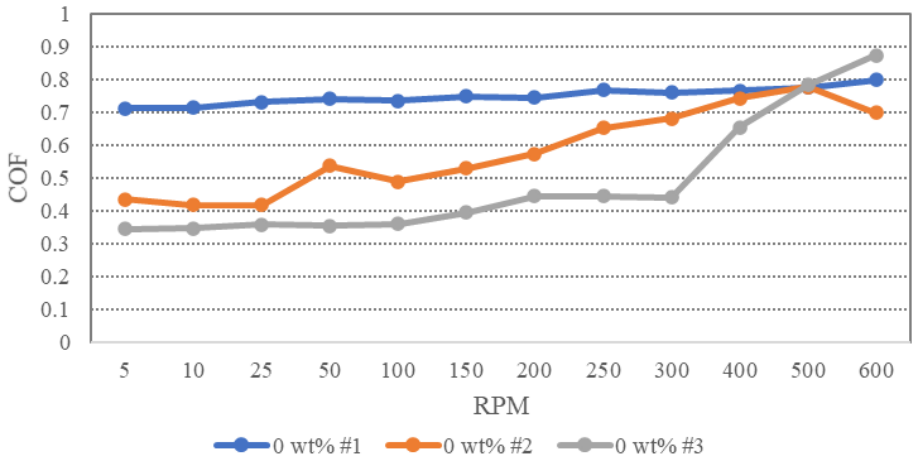

Figure 3.3: Stribeck curves from 0 wt% on silver samples. Each point is the average COF over the 3 minutes at that speed

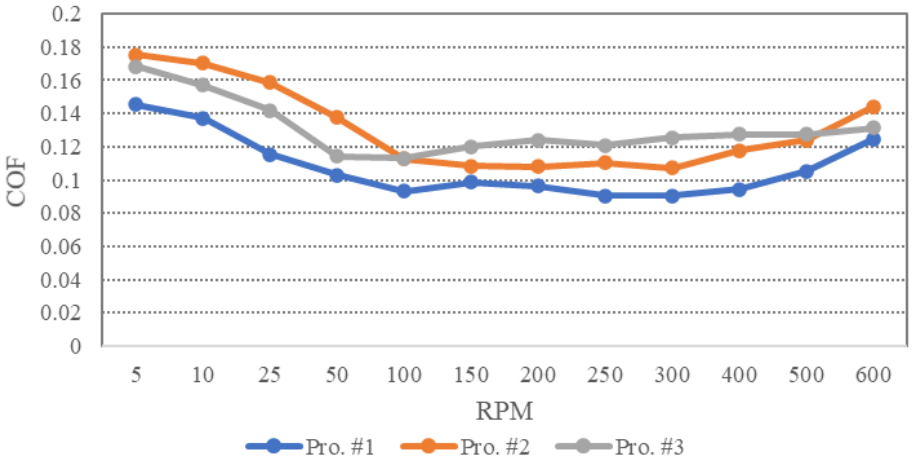

Figure 3.4: Stribeck curves for proprietary lubricant on silver samples

Similar to the tests for proprietary lubricant on silver samples, the proprietary lubricant on gold samples also produced more typical-looking Stribeck curves, along with good run-to-run consistency (see Fig. 3.5). The primary difference is that the gold features a more pronounced COF jump at high speeds, perhaps due to the lubricant film being 'plowed' through at the start of the experiment along with gold being a softer material than silver.

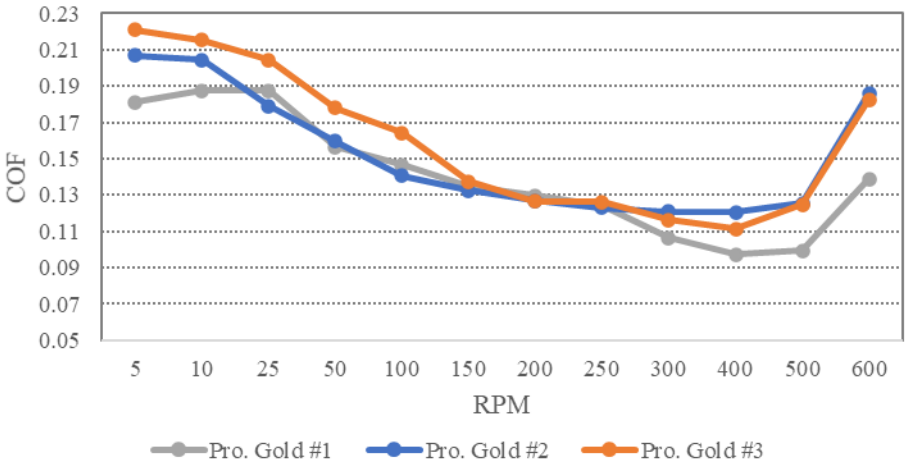

Figure 3.5: Stribeck curves for proprietary (Pro.) lubricant on gold samples

As discussed in Ch. 2, silver nanoparticles were introduced to the proprietary lubricant via modifying the solvent (that is, the solvent designed to evaporate and leave the lubricant film behind). The particles were prepared within the solvent and the resulting colloid ('proprietary solvent colloid') was mixed with the proprietary lubricant prior to application (resulting in the 'proprietary colloid'). Particles were left in the lubricant film after the solvent evaporated. The Stribeck curves for the proprietary colloid on silver samples had slightly more variance between, and even within, tests (Fig. 3.6). As the proprietary colloid had precipitation instability issues (Ch. 6), some curves were excluded in the final set used for averaging (the cases included are shown in Fig. 3.7) to ensure consistent experiment conditions were used for comparison. However, friction was consistently low, and the overall shape of the curves still resemble that of a typical Stribeck curve.

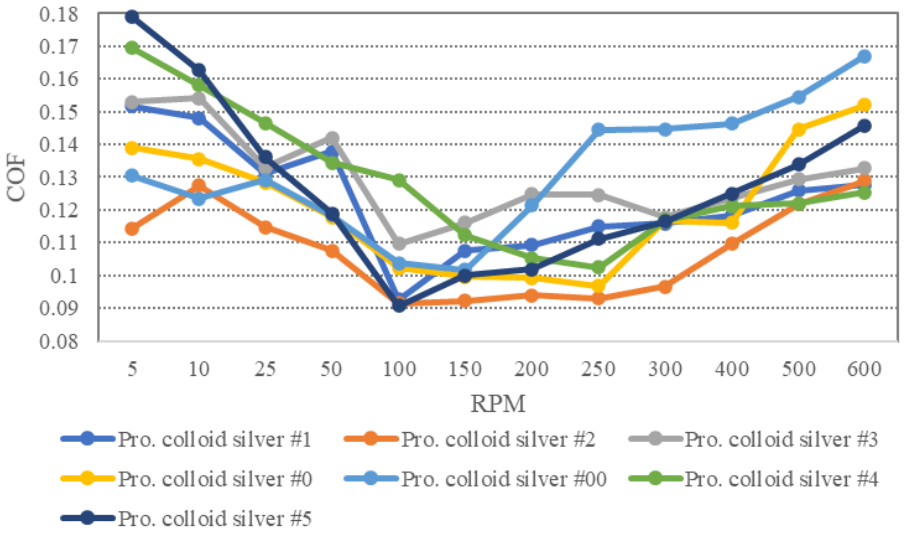

Figure 3.6: All Stribeck curves for the proprietary colloid on silver samples

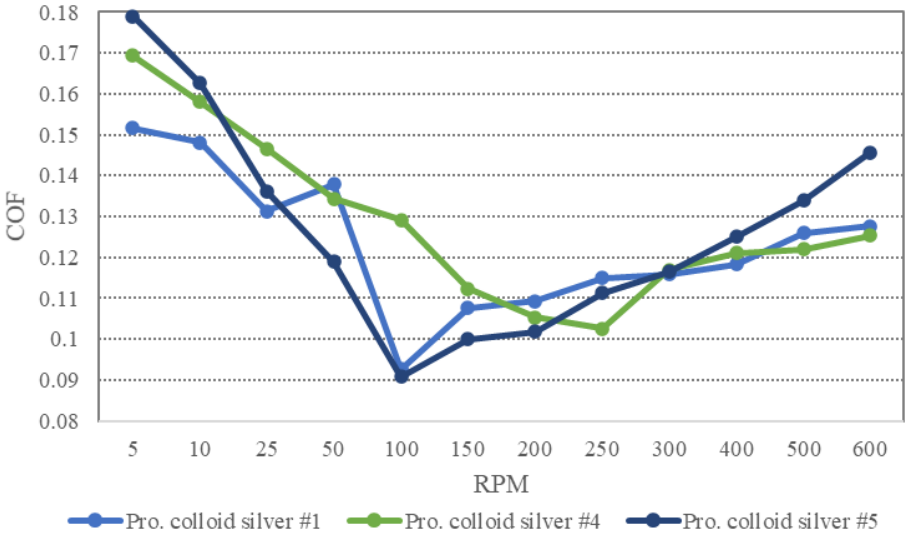

Figure 3.7: Selected Stribeck curves for averaging and comparison

A couple of Stribeck tests were conducted using the proprietary solvent colloid for comparison to the proprietary colloid results. As this was not a full lubricant, only two tests were performed for exploration. The experiment procedure was the same as for the lubricants, with a 24-hour drying period. There were no obvious stability issues with the solvent at the time; however, since these tests, some stability issues seem to have arisen, as mentioned in Ch. 2 and further discussed in Ch. 6.

As might be expected from a substance not designed to be a lubricant, the resulting curves do not resemble the typical Stribeck curve (see Fig. 3.8). However, the COF remained low overall, with a distinct increase in friction below 150 RPM and some slight decrease going from 10 RPM to 5 RPM. It is known from prior research that even dry particles alone can lower friction so long as they remain present within the contact [17]. Since the film left after evaporation of the proprietary solvent colloid is likely largely particles (and stabilizer) alone, the lower friction (as compared to pure dodecane or dry contact) is likely mostly due to the particles.

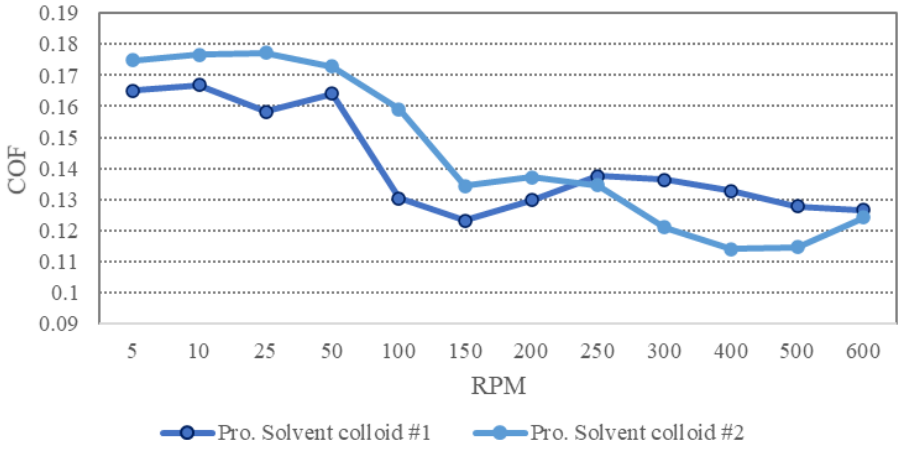

Figure 3.8: Stribeck curves from proprietary solvent colloid on silver samples

The proprietary colloid on gold samples produced results with very good run-to-run consistency (see Fig. 3.9). These curves closely resemble the typical Stribeck curve and feature the most consistently extreme rise in friction at low speeds of any of the tested lubricants. Given that these tests feature wider wear scars than the proprietary lubricant on gold, indicating higher wear, perhaps this dramatic rise is a result of thin gold-film effects as the plated gold layer is worn down and the underlying nickel barrier layer becomes more dominant in the friction [28].

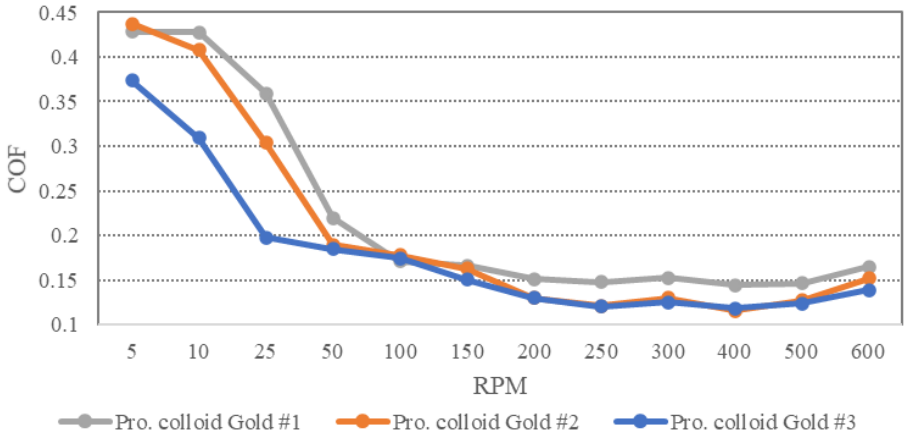

Figure 3.9: Stribeck curves from proprietary colloid on gold samples

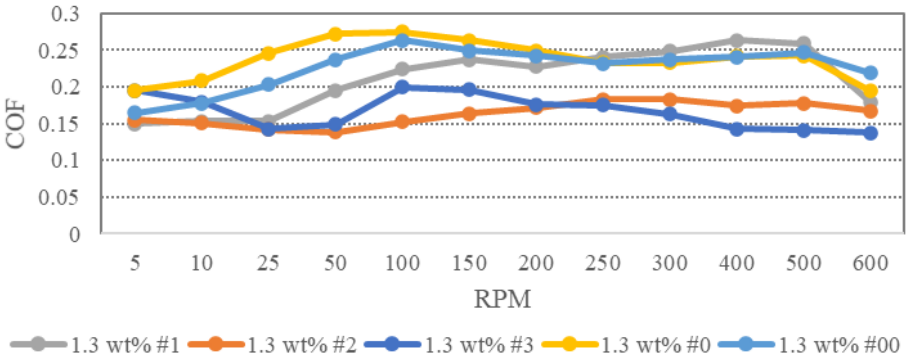

Figure 3.10: All 1.3 wt% Stribeck tests

The 1.3 wt% dodecane colloids produced relatively flat friction curves, more comparable to those generated by the pure dodecane than a typical Stribeck curve (see Fig. 3.10). Given changes in test procedure following the discovery of the (soon to be discussed) outlying Stribeck curves with the dilutions, only the later three of these curves are used for the final average and comparison (see Fig. 3.11).

Most of the dodecane nanolubricant curves feature an odd trend at lower speeds: the COF drops. This is so extreme that in some cases the COF was lower than at the highest speeds; given that contact area usually increases with decreasing speed due to the loss of any possible fluid film separating the surfaces, this is a highly unusual result. Notably, this effect was not consistently seen in the 1.3 wt% on gold samples (Fig. 3.12), nor in the

proprietary colloids. This lower COF trend is what prompted the forthcoming constant speed tests, where the trend was confirmed on silver samples. Presuming that this drop in COF at lower speeds is a result of some novel way that the lubricant interacts with certain materials, this could be useful for applications requiring low friction at lower speeds, like possibly in EVs, as the common use of low viscosity lubricants results in high friction at low speeds for them [23]. Further investigation into this phenomenon should be conducted in the future.

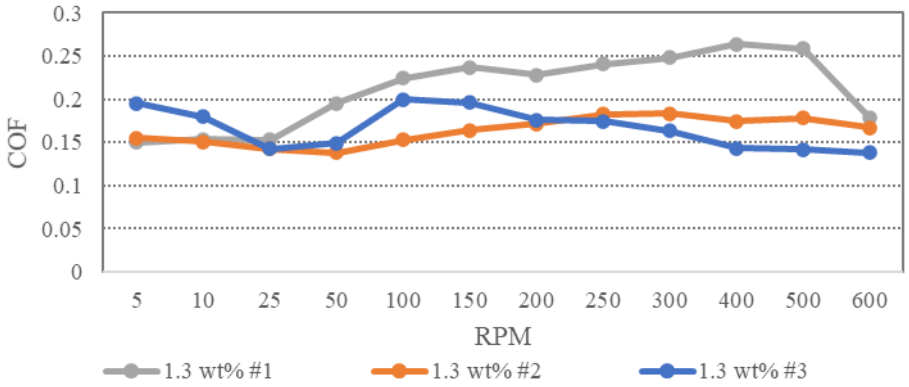

Figure 3.11: Selected 1.3 wt% Stribeck tests

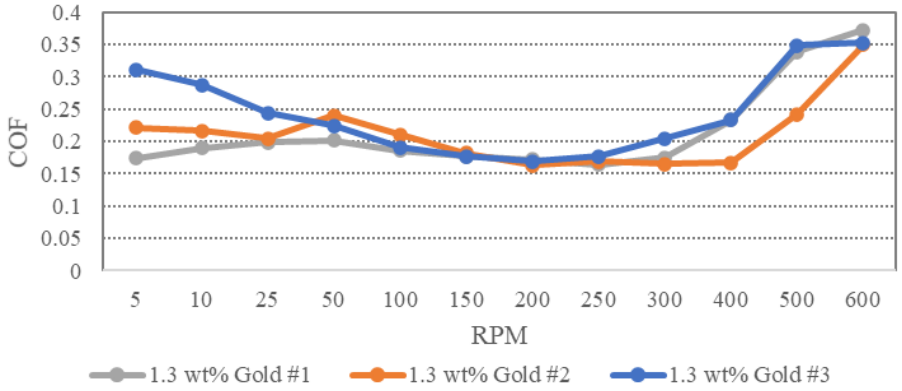

Figure 3.12: Stribeck curves from 1.3 wt% on gold samples

Dilutions and Outliers

As prior research indicated that the concentration of nanoparticles directly impacts the friction and wear behavior [8-10, 17], several dilutions of the dodecane nanolubricant were made to explore these effects. As before, at least three tests were run for each dilution. Early tests of the dilutions featured outlying curves (see Fig. 3.13-3.15) with much higher friction. Further tests showed that the lower friction values were reflective of the typical behavior of the lubricants, with additional evidence supporting this conclusion coming from the SEM and EDS analysis (Ch. 5). As such, the outlying curves were not used in the final averages and comparisons. However, these outlying tests were further investigated to see what might have prompted such stark differences in both friction and wear behavior, as discussed further in Ch. 5.

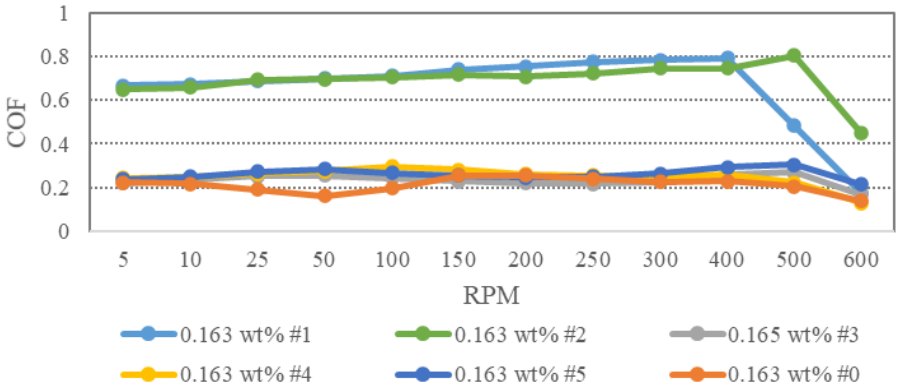

Figure 3.13: 0.163 wt% Stribeck curves, including outliers

The curves for the 0.65 wt% and 0.163 wt% dilutions both feature good run-to-run consistency and low friction values (see Fig. 3.16, 3.17). Both additionally feature a pronounced drop in COF at low RPM, where 0.65 wt% is the most extreme example. Though the lowered friction at low speeds is odd, the rest of the curves do somewhat resemble a typical Stribeck curve, besides a sharp drop in friction at 500-600 RPM. The

Stribeck curves for 0.325 wt% have more run-to-run variance than the 0.65 wt% or 0.163 wt% curves (see Fig. 3.18).

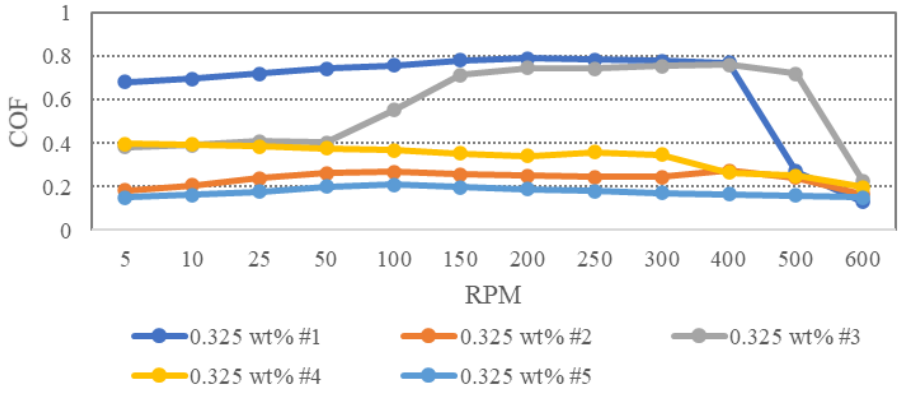

Figure 3.14: 0.325 wt% Stribeck curves, including outliers

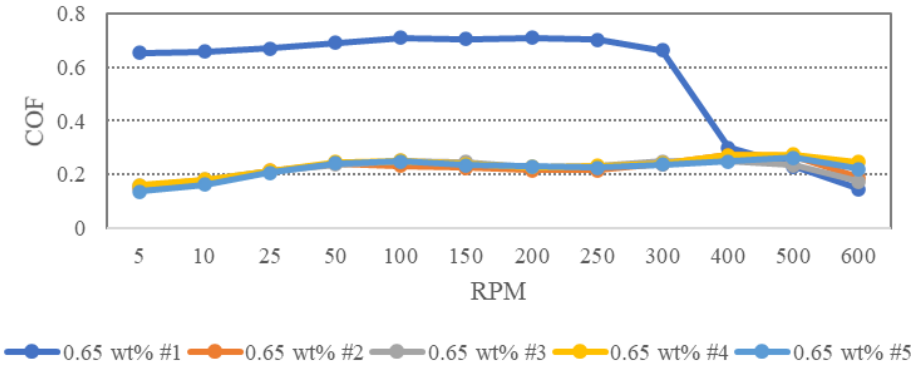

Figure 3.15: 0.65 wt% Stribeck curves, including outliers

The outlying curves (henceforth known as 'the outliers') all feature sharp jumps in COF for speeds lower than 300-400 RPM. For all but one 0.325 wt% outlier, once the jump in friction occurs, it does not lower again for the duration of the test. To compare these outliers directly, the portions of the curves lower than 400 RPM were plotted on a single graph (see Fig. 3.19). Rather interestingly, the higher COF values were very similar between all the particle concentrations, indicating that this is likely close to the underlying dry friction levels between the surfaces. Typical metal-on-metal kinetic COF values are between ~0.2-0.8 [29], so it would fit, though this varies widely based on geometry,

loading, etc. A 25 RPM dry contact test conducted with a silver sample set produced an average COF of 0.7985, though this includes sliding on the bronze core and was only a single test. This value is above the average levels of the outliers at 25 RPM as well. Given that the outliers have less severe wear, fully dry contact was unlikely present with them.

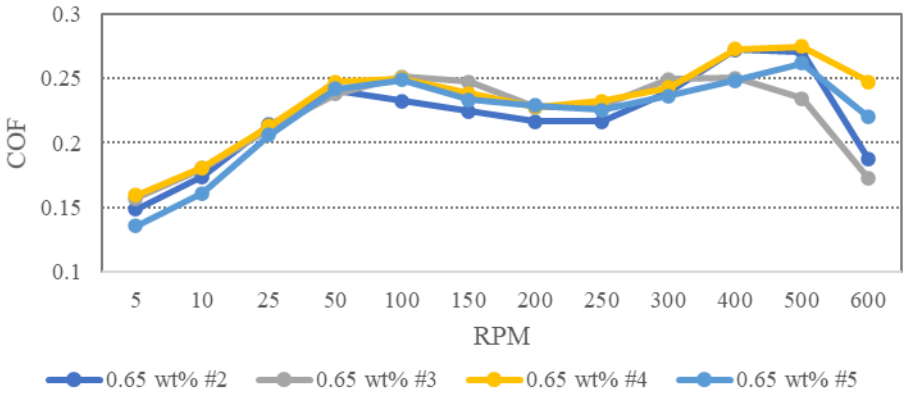

Figure 3.16: 0.65 wt% Stribeck curves used for averaging and later comparison

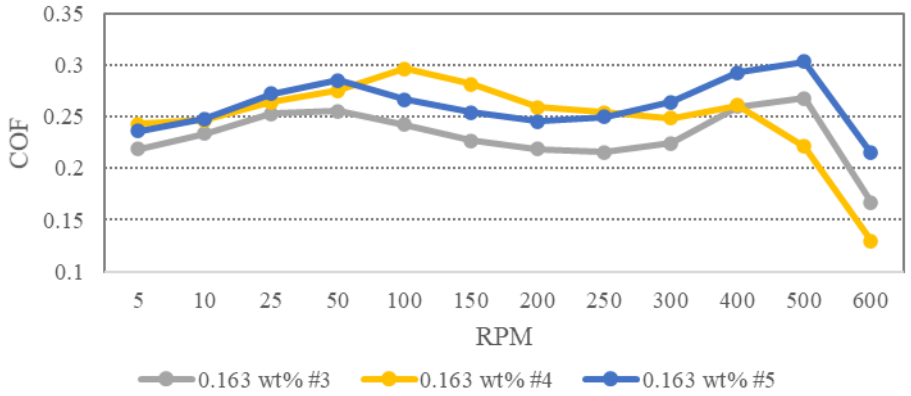

Figure 3.17: 0.163 wt% Stribeck curves used for averaging and later comparison

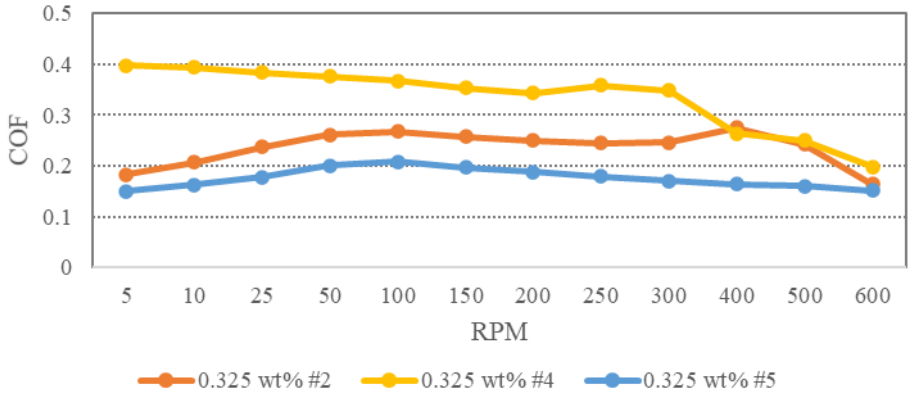

Figure 3.18: 0.325 wt% Stribeck curves used for averaging and later comparison

All outliers feature significantly wider (and deeper, as seen in SEM, Ch. 5) wear scars in addition to higher friction. A possible hypothesis as to the cause of these results is the collapse of the meniscus between pin and flat (Fig. 3.20) at some point during the test. This would hypothetically result in a lack of both lubricant and particles within the contact and corresponding higher friction values. However, this does not explain the resumption of lowered friction on the single 0.325 wt% outlier. Interestingly, below 300 RPM, the high friction outlier branch is close to the friction levels of one of the pure dodecane (0 wt%) Stribeck tests, while the single 0.325 wt% run which returns to lower friction does so at a level similar to the other two 0 wt% runs (see Fig. 3.21).

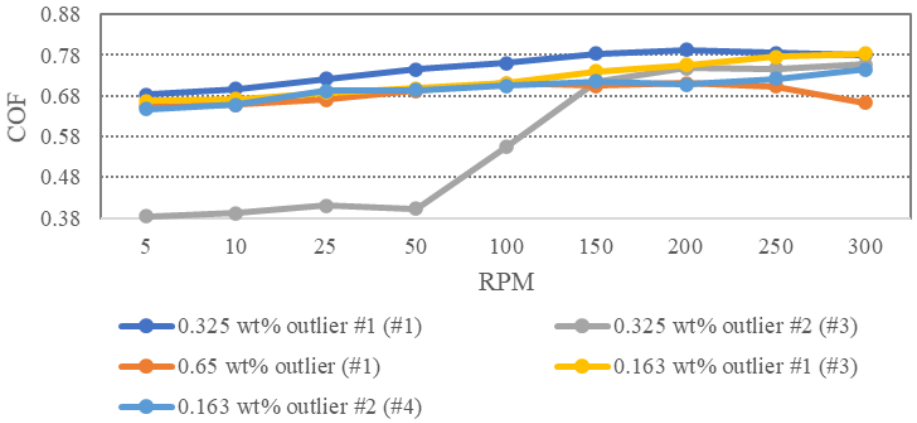

Figure 3.19: Comparison of the outliers starting at 300 RPM

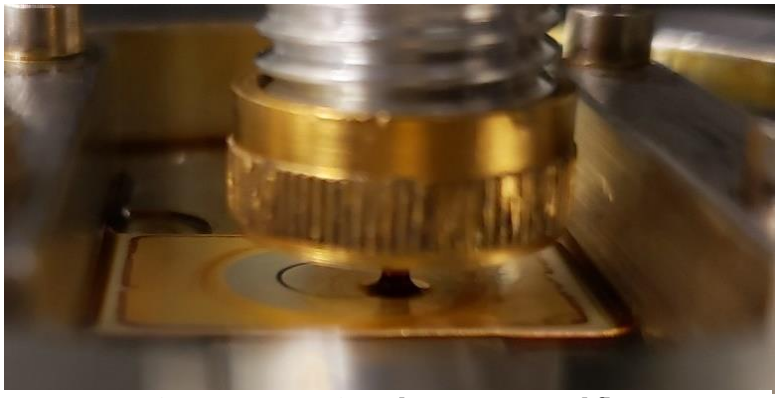

Figure 3.20: Meniscus between cap and flat

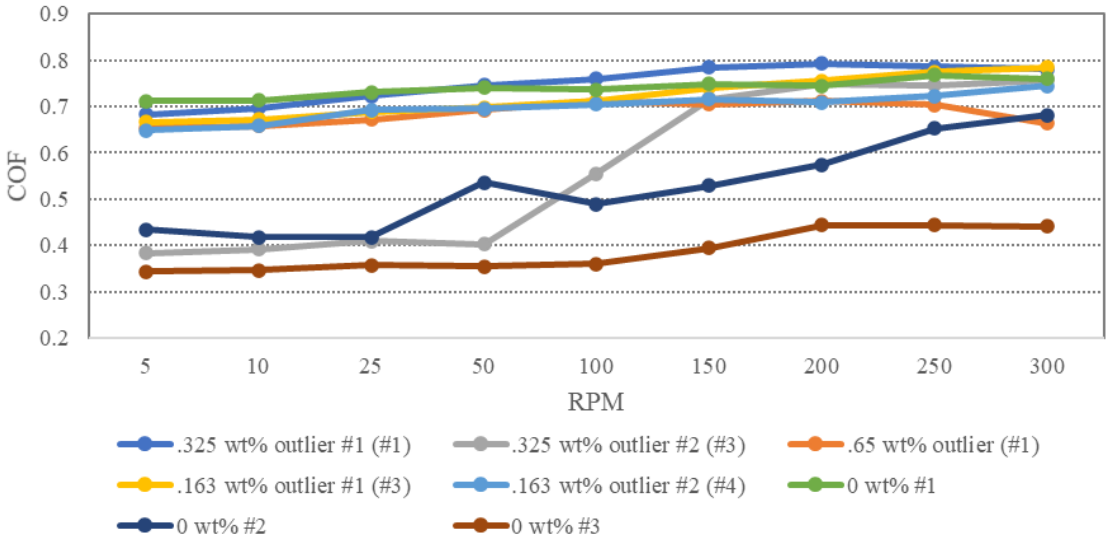

Figure 3.21: Adding the 0 wt% curves (below 300 RPM) to Fig. 3.19 curves for comparison

The friction levels being close to pure dodecane would indicate the possibility of some odd phenomena causing the particles to entirely (or nearly entirely) vacate the contact while pure (or mostly pure) dodecane is left behind. This would be similar to friction increases due to particles vacating a dry contact [17]. It is initially difficult to see how this would transpire while there is dodecane left on the surface, as it would theoretically ensure that particles are continually transported back into the contact. However, given the visible ring of lowered lubricant presence around the wear scar in Fig. 3.20, perhaps a severe collapse of the meniscus would allow the particle levels to drop low enough to negate much (or all) of their effect on friction. This could also be related to the transparency of the lubricant film on the flat samples after 24hrs (see Fig. 6.13a, Ch. 6). Alternatively, a collapse of the meniscus could result in enough lubricant escaping for the contact to become starved/near dry, resulting in higher friction.

Overall Stribeck Comparisons and Discussion

Overall, 7 different lubricants were each tested at least three times under uniform conditions. One ‘proprietary solvent colloid’ was also tested twice, though it is excluded from the coming comparisons as it was not a lubricant. Every average Stribeck curve may be seen in Fig. 3.22 (note: unless stated to be gold, the test was on a silver sample).

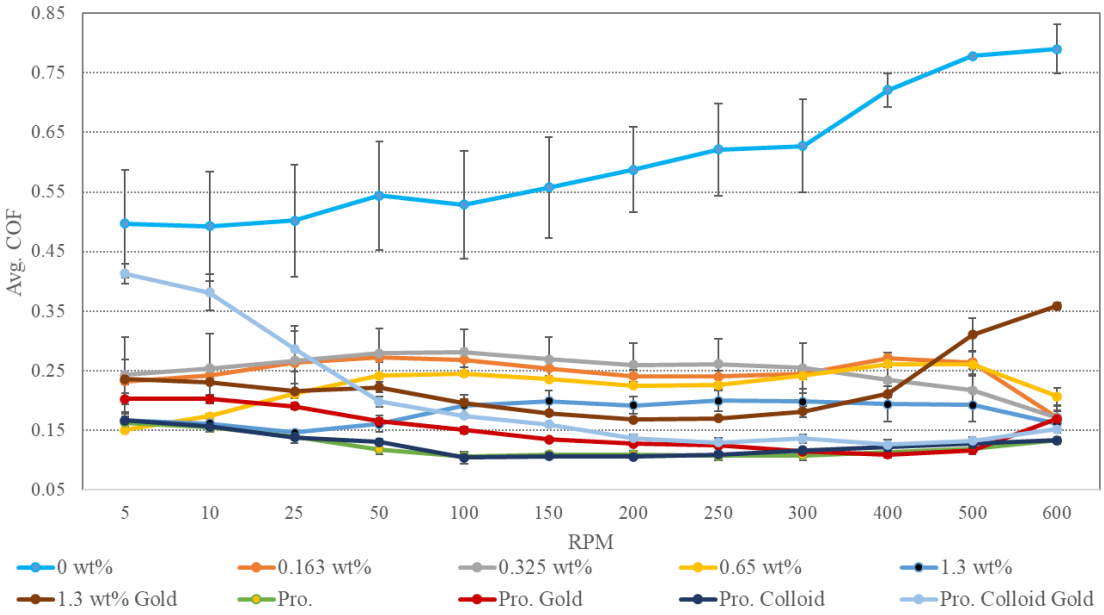

Figure 3.22: All Stribeck curves compared (silver samples used unless noted to be gold) with standard error for error bars

From Fig. 3.22, it is obvious that the 0 wt%/pure dodecane as tested on silver samples has the highest friction values of any tested lubricant. Meanwhile, the proprietary lubricant tested on silver forms much of the lower friction boundary, while almost every nanoparticle lubricant offers significantly lower friction vs the pure dodecane. Notably, the friction of the ‘proprietary colloid’ on gold samples approaches the levels of friction seen in the pure dodecane on silver when operating at 5-10 RPM. More detailed comparison of the lubricants, however, requires separate inspection of the different lubricant groups while

excluding the 0 wt%/pure dodecane for clarity. Fig. 3.23 & 3.24 feature the nanolubricants on silver.

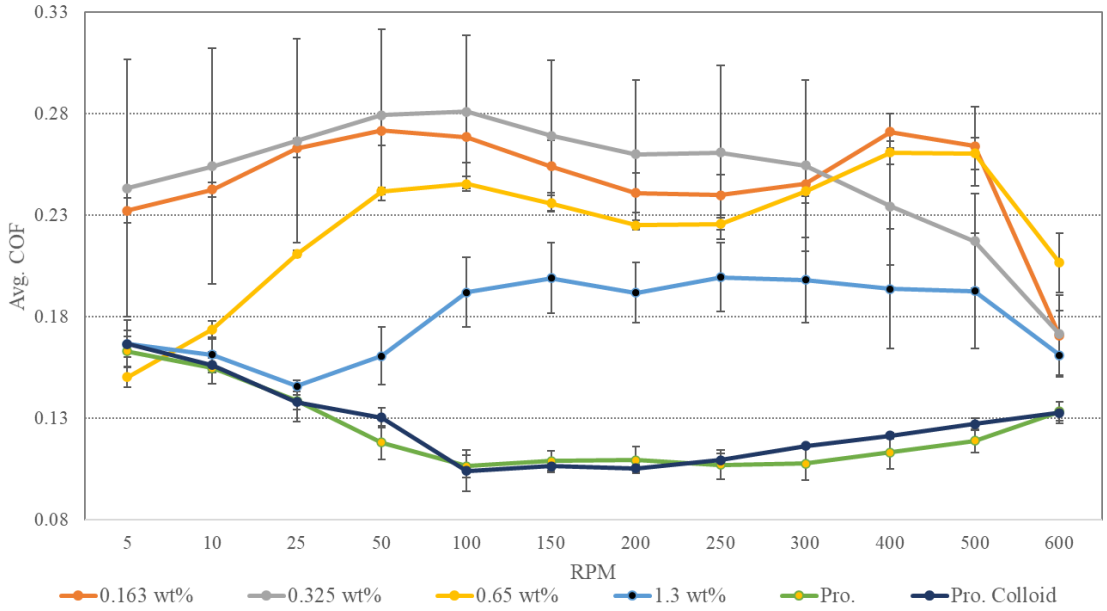

Figure 3.23: Nanolubricant Stribeck curves from silver samples

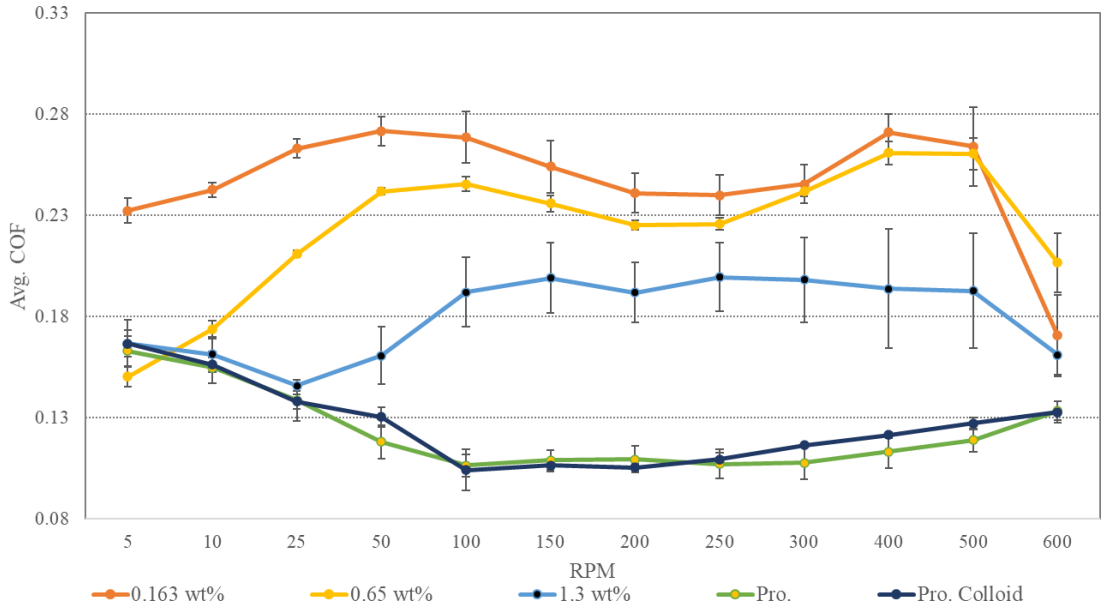

Figure 3.24: Nanolubricant Stribeck curves from silver samples (excluding 0.325 wt%)

Given the previously seen variability in the 0.325 wt% tests (Fig. 3.18), the error bars are correspondingly large. Thus, Fig. 3.24 removes it for the sake of a clearer comparison of the other lubricants.

For the dodecane nanolubricants, particle concentration changes the friction level. Except for 0.325 wt%, a trend where lower particle concentrations are near inversely proportional to friction levels is present, which fits with prior research [8-10, 17]. Of note, on silver samples the 1.3 wt% lubricant nearly matches the friction performance of the proprietary lubricant at speeds of 25 RPM and lower (Fig. 3.24). The proprietary colloid features very similar friction levels to the proprietary lubricant except between 100-200 RPM, where it features slightly lower friction.

Although the primary reason for performing gold sample tests was to investigate if the silver nanoparticles would attach to the surface during testing, the friction results are still of interest. Generally, the gold samples have higher friction than their silver counterparts (see Fig. 3.25), possibly due in part to gold being a softer metal. Interestingly, the usual friction improvements seen with nanoparticles do not appear when comparing the proprietary lubricant and proprietary colloid on gold; in fact, the colloid features higher (MUCH higher, below 50 RPM) friction values (see Fig. 3.26).

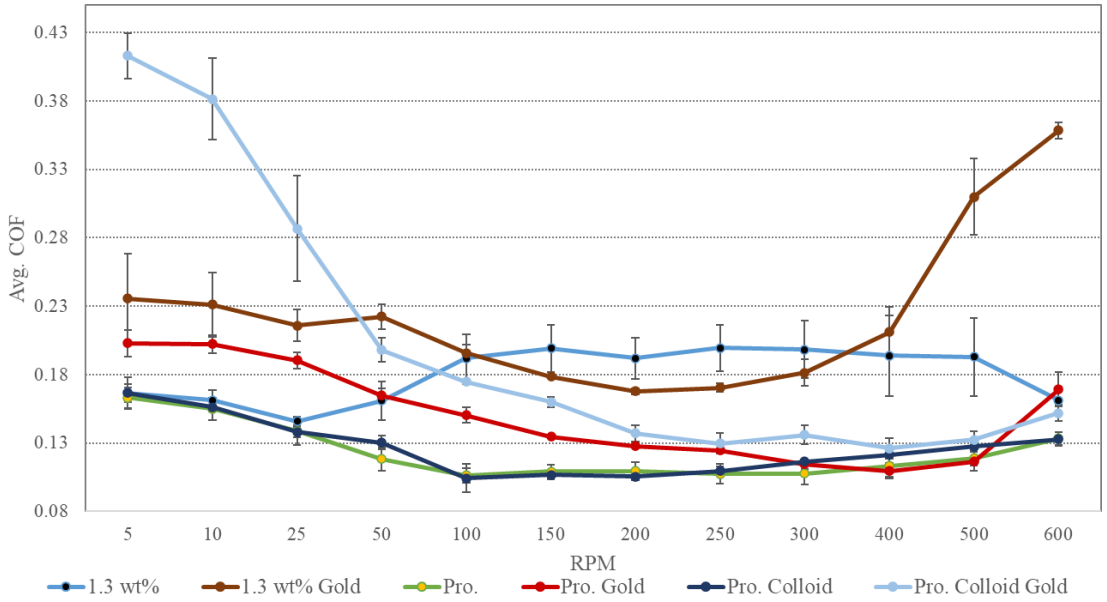

Figure 3.25: Comparison of silver/gold sample Stribeck tests

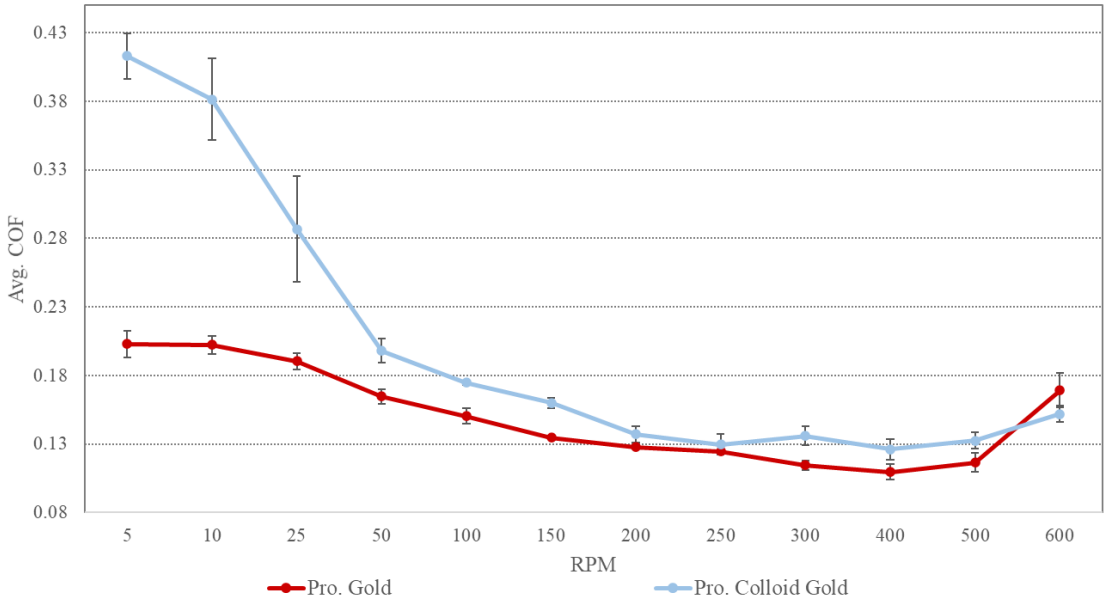

Figure 3.26: Comparison of Proprietary lubricant and Proprietary colloid on gold

Constant Speed Tests

As mentioned previously, an unusual trend was observed with most of the dodecane silver sample Stribeck tests: that of the friction dropping significantly at lower speeds (particularly <50 RPM). Given that this is a very unusual phenomenon, constant speed tests

were conducted to investigate. These were performed at both 10 and 25 RPM, with three tests performed at each speed. All tests (except for a single dry test at 25 RPM) were done using either the 1.3 wt% nanolubricant or the proprietary lubricant (for comparison) on silver samples. These tests were run long enough to ensure that they covered the same number of rotations as the full Stribeck test: 7770 revolutions. This equated to a runtime of 777 min for 10 RPM and 310.8 min for 25 RPM.

For the 1.3 wt% nanolubricant, all three 10 RPM tests and two of the three 25 RPM tests featured friction at two different levels: during a possible 'run-in' period ('Initial' region), and a possible 'Worn-in' region (see Fig. 3.27 for a representative example). The time taken before the friction changed varied between experiments, and there was no corresponding change to the Bruker ECR readings to match.

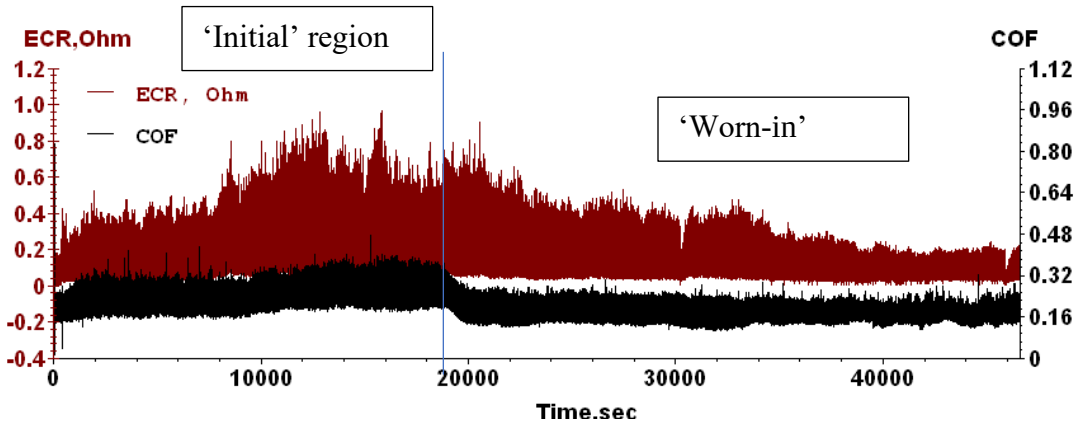

Figure 3.27: 1.3 wt% 10 RPM COF/Bruker ECR data

To make a comparison to the Stribeck curve averages, the COF from each of the aforementioned regions of data ('Initial' and 'Worn-in') was averaged using MATLAB (script in appendix A). This was done for each test featuring this effect; the average of these

was then taken for the separate tests. These results were then compared to the corresponding average COF values from the Stribeck curve (see Table 3.1).

Table 3.1: Comparison of constant speed and Stribeck COF values, 1.3 wt%

Speed (RPM)	Initial COF	Worn-in COF	Stribeck COF
10	.2287	.1753	.1613
25	.2972	.1812	.1460

It should be noted that the 25 RPM Worn-in value was averaged from two tests as one did not feature a drop in friction. The Worn-in COF values are slightly higher than their Stribeck test counterparts. While the 1.3 wt% averages from the Stribeck curve do not indicate a decrease between 10 and 25 RPM, it can be seen back in Fig. 3.23 and 3.24 that the average 1.3 wt% curve is the outlier among the dodecane nanolubricants in that regard. Additionally, the COF drops when going from 25 RPM to 10 RPM regardless of being in the Initial or Worn-in region, indicating that the decrease in friction present in the Stribeck curves could still have some relation to the dodecane nanolubricant lubricant itself interacting with the silver samples.

The significant COF drop seen within each 1.3 wt% constant speed test fits with the idea that the COF change in the Stribeck curves is a result of a change from silver-on-silver to silver-on-nickel sliding. As further discussed in Ch. 5, the SEM/EDS results generally show that the caps have the silver plating worn off with the nanolubricants even if the plates maintain a silver coating, so it is a probable cause. However, these same results show that the outliers feature silver transfer from the plate to the pin, exposing nickel on the plate and resulting in silver-on-nickel sliding, yet these do not have lowered friction levels. Perhaps, then, polishing or burnishing of the plate surface also plays a role. There

are likely competing effects at work, possibly including a specific effect of the lubricant on the silver samples, with a dominant cause being difficult to ascertain.

The constant speed tests of the proprietary lubricant on silver samples, by contrast, have higher friction at lower speeds (Table 3.2) as is typical. The COF also did not feature consistent variations within tests like the 1.3wt% lubricant, instead remaining largely steady throughout. The average constant friction values are similar to their Stribeck counterparts, being higher at 10 RPM and lower at 25.

Table 3.2: Comparison of constant speed and Stribeck COF values, Proprietary

Speed (RPM)	COF	Stribeck COF
10	.1841	.1630
25	.1461	.1549

Wear Observations

In all the well-behaved nanolubricant tests, the plate wear scar was not deep enough to be discernable in stylus profilometry data, indicating that the wear scar was of a depth similar to the existing surface roughness and likely did not make it through the silver plating by any significant amount. This was later confirmed by SEM/EDS analysis (Ch. 5).

Additionally, none of the tests (besides the single 25 RPM dry test) caused a measurable change in sample plate/cap mass (though our analytical scale is limited to a resolution of 0.1 mg). Therefore, to characterize the wear, an optical microscope and calibration slide were employed. Each sample had its scar width measured, and the average was calculated for each set of test conditions. The standard error was calculated from these

width measurements and used for the error bars in the comparison charts (See Fig. 3.28-3.29).

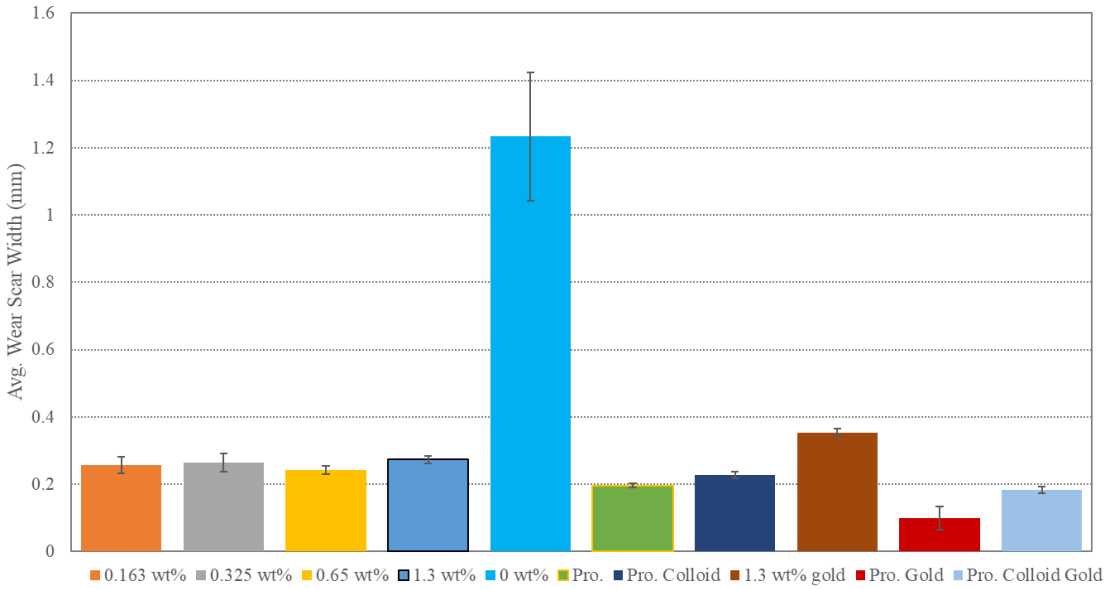

Figure 3.28: Comparison of average wear scar widths, test on silver unless noted

As would be expected given the high and variable friction, the 0 wt% dodecane featured the most severe and varied scar widths (Fig. 3.28); it is enough of an outlier to make its removal necessary for the comparison of the other lubricants (Fig. 3.29). Adding particles to the proprietary lubricant (to get the proprietary or 'Pro.' colloid) resulted in wider scars than found with the proprietary lubricant, while the addition of particles to dodecane produced smaller scar widths as compared to the unmodified dodecane in every test on silver samples. The dodecane nanolubricants tended to result in higher wear than the proprietary lubricant. However, a lot of electrical contacts use materials that develop oxide layers and are designed to wipe/scrape them off upon connection/disconnection [30], even occasionally requiring surface forces of 5-10 N in the process [31]; for some applications, like aluminum power connectors, abrasive particles are even commonly

introduced into the contact to break through the oxide layers that often develop [32]. Thus, this higher wear could be advantageous for certain applications.

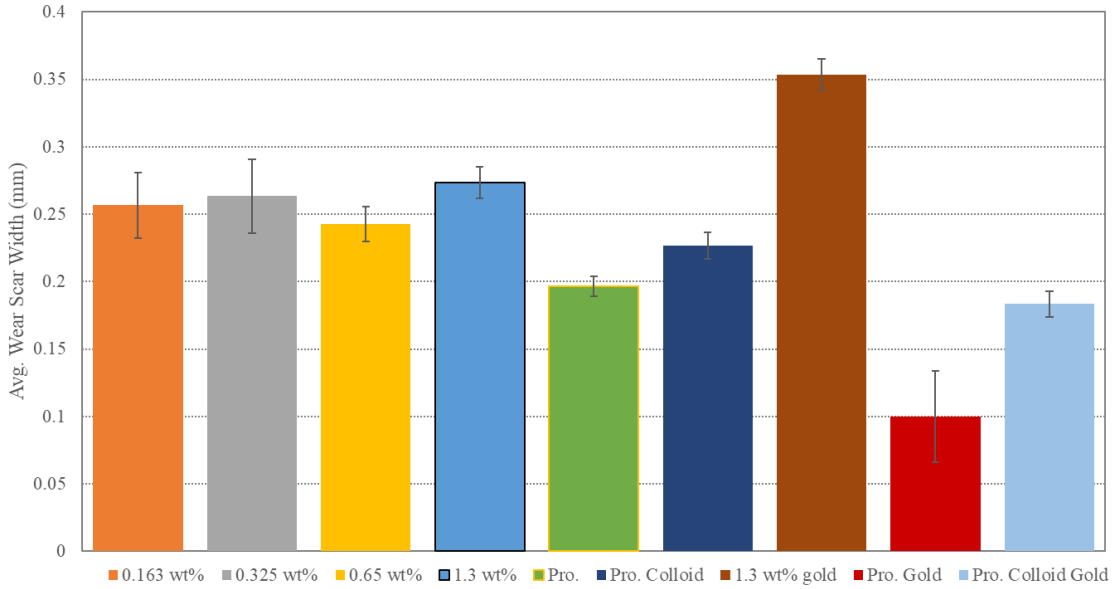

Figure 3.29: Comparison of average scar widths, excluding 0 wt%; silver test unless noted

Despite the friction levels nearly being inversely proportional to particle concentration, there does not appear to be a similarly well-defined trend in wear scar widths. However, as is seen and discussed in Ch. 5, decreasing the particle concentration did result in slight exposure of the nickel barrier layer among the silver plate samples, indicating that wear does depend on particle concentration.

The best performance, in terms of average scar width, was the proprietary lubricant on gold samples. There was a slightly higher than usual variance in scar widths, however. The 1.3 wt% nanolubricant, when used on gold, produced slightly higher friction than the proprietary lubricant and also the widest wear scars seen outside of the dry or 0 wt% tests on silver.

When adding particles to the proprietary lubricant, they appear to result in slightly wider wear scars. Friction levels are nearly the same as the proprietary lubricant if silver samples are used, while friction is far higher at speeds below 50 RPM on the gold samples. This wear increase is likely due to the fact the particles are abrasive; since nanoparticles generally have higher yield strengths than their bulk material equivalents [3, 4], it is logical that higher abrasive wear would result from their addition to a lubricant.

Overall, the scar widths for all lubricants besides 0 wt%/pure dodecane are quite consistent for tests in the boundary regime. It is not uncommon to see wear vary by orders of magnitude in the boundary regime, after all. Adding particles to the dodecane made the lubricant competitive with the proprietary lubricant in terms of wear (and friction below 25 RPM) under these test conditions.

Chapter 4–Results: Electrical Contact Resistance

The characterization of the electrical contact resistance (ECR) changes across the various friction/wear tests described in Ch. 3 was another goal of this research. Attempting this proved to be a difficult task, as there was significant noise and very little repeatability to be found in these measurements despite the best efforts to ensure consistent and stable test conditions.

All the ECR measurements used in this comparison were recorded by a computer connected to an Agilent 34410A DMM set to collect data with an integration of "100 PLC" for the highest resolution. Here, "PLC" refers to "Power Line Cycles", indicating that the DC measurement was integrated over 100 cycles of the power grid to reduce noise [33]. This resulted in an automatically set ECR sample rate of ~0.29 Hz. Repeatability of the resistance measurement was confirmed across the removal and reattachment of the wires on multiple occasions and sample sets; though it was found that in some rare cases it could take 5-10 minutes before the ECR returned to the previously measured value. Thus, as there was a risk of the dodecane lubricants 'drying' during any potential extended measurement period, efforts were made to ensure that the wires always remained attached to the sample fixtures outside of tests.

A Keithley 2001 DMM was also employed for comparison in some tests, as it had higher resolution, however it could not be attached to the computer to download and/or record data sets. As a result, data from it had to be taken by hand. The output of this DMM was usually quite noisy and prone to rapid fluctuations, however, and this combined with attempting to record data by hand resulted in low quality data which has not been used for

comparisons. Most tests do not have this data, instead opting for only collecting the Agilent DMM data.

In general, for each set of ECR measurements, the goal was a set of 90 consecutive measurements with relative consistency; however, in nearly all cases at least 120 measurements (across ~6.5 minutes) were collected, as the initial set (~30, in most cases) featured some form of transient resistance changes before leveling off (Fig. 4.1 is an example). This occurred without correlation to the contact being dry or lubricated and did not change between lubricants; thus, it is unlikely to be a result of primarily squeeze-film effects. Though, when the transient effect was a slight decrease (Fig. 4.1) occurring with a lubricated contact, it might fit with prior research [34]. On rare occasions (generally after reattaching the wires to record the ECR after a test), more than 120 measurements were required to meet the 90-measurement goal.

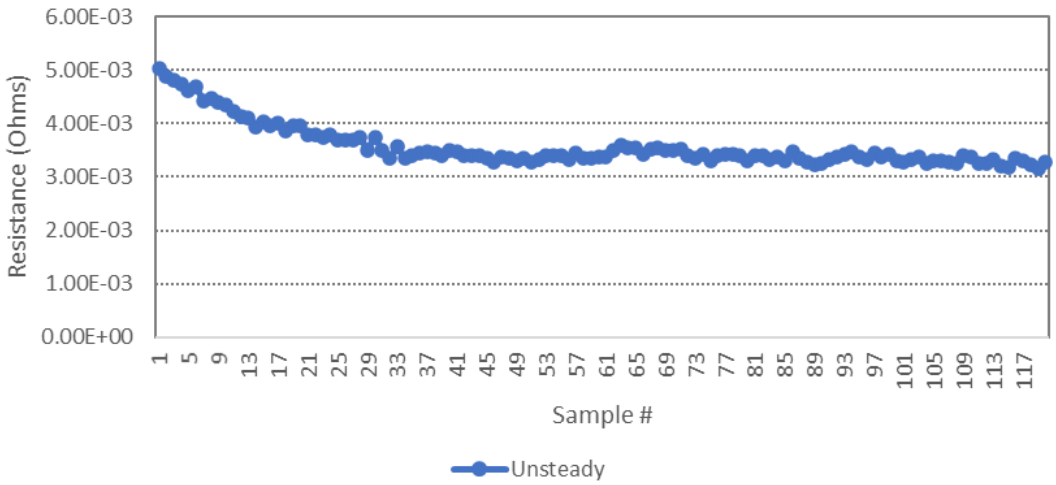

Figure 4.1: An example of initial samples having a transient change, in this case a decrease

ECR comparisons were based off the averages of the sets of 90 samples from each test stage (‘dry’, ‘wet’, ‘after’). As mentioned in Ch. 1, since a large change in ECR across a contact can result in an unacceptable ECR level for a given application and be cause for contact/connector failure, the area of interest here was the change in ECR across the tests. To obtain the change in ECR, the difference between the average of ECR measurements taken immediately before testing and after lubricant application (or 24hr of lubricant drying, for proprietary-based lubricants) and after the test was calculated. However, this could result in both increases or decreases in ECR within tests of a single lubricant, indicating competing mechanisms are present. Since the primary goal was to find the magnitude of the change, regardless of direction, the absolute value was taken for each average ECR change calculated.

The average of these ECR change magnitudes was taken (like the averaging of the COF data) for each set of tests, yielding an overall average ECR change magnitude for comparisons between the various lubricants and test procedures. Error bars were included when applicable by calculating the standard error of the average ECR change values. A full comparison of these ECR changes, including those from the outlier Stribeck tests described in Ch. 3, may be seen in Fig. 4.2.

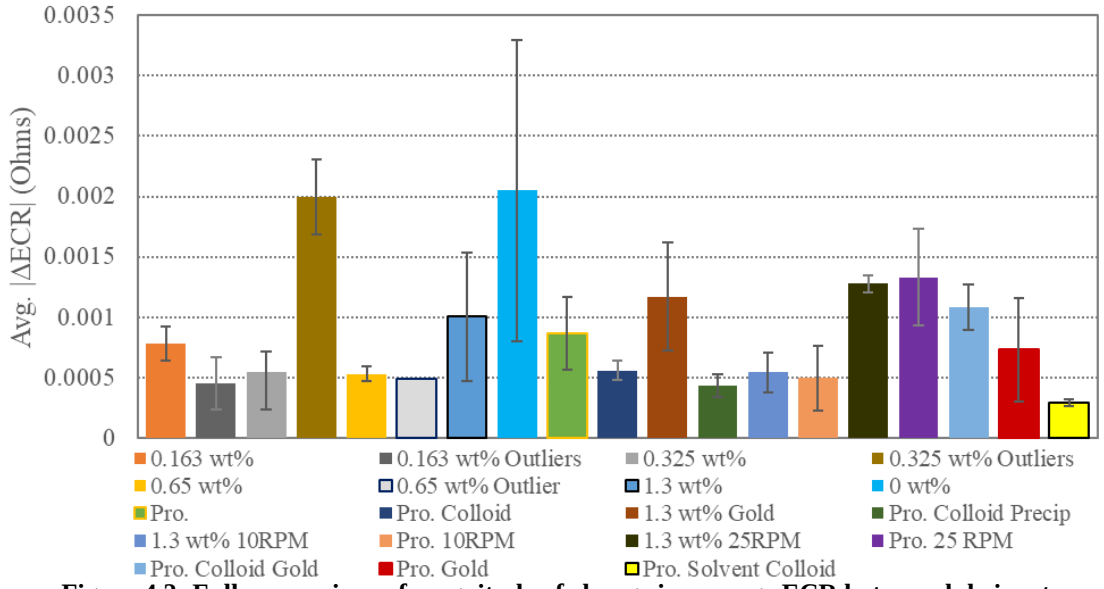

Figure 4.2: Full comparison of magnitude of change in average ECR between lubricant application and after test

Not much can be easily ascertained from Fig. 4.2 besides 0 wt% having both the highest average change in ECR and the largest uncertainty, just as in the friction and wear results. Only the 0.325 wt% outliers are close in magnitude to 0 wt%. However, it can be seen that many of the average ECR changes are under 1 mΩ in magnitude and are thus relatively minor (perhaps even within the magnitude of noise for many applications). Further comparisons require separation of the data into multiple figures (Fig. 4.3-4.6).

The main areas of interest regarding the ECR change data are: what effect does particle concentration have, if any, on the average change in ECR and how do they compare to proprietary & dodecane lubricants? Are there differences in average ECR change between gold & silver tests? Are there differences between the well behaved and the outlying Stribeck tests, or between the Stribeck and the continuous speed tests? What effect does the addition of particles to the proprietary lubricant have? Fig. 4.3 begins by

comparing the average change in ECR between the dodecane nanolubricant concentrations (not including outliers) and the proprietary lubricants from the Stribeck tests.

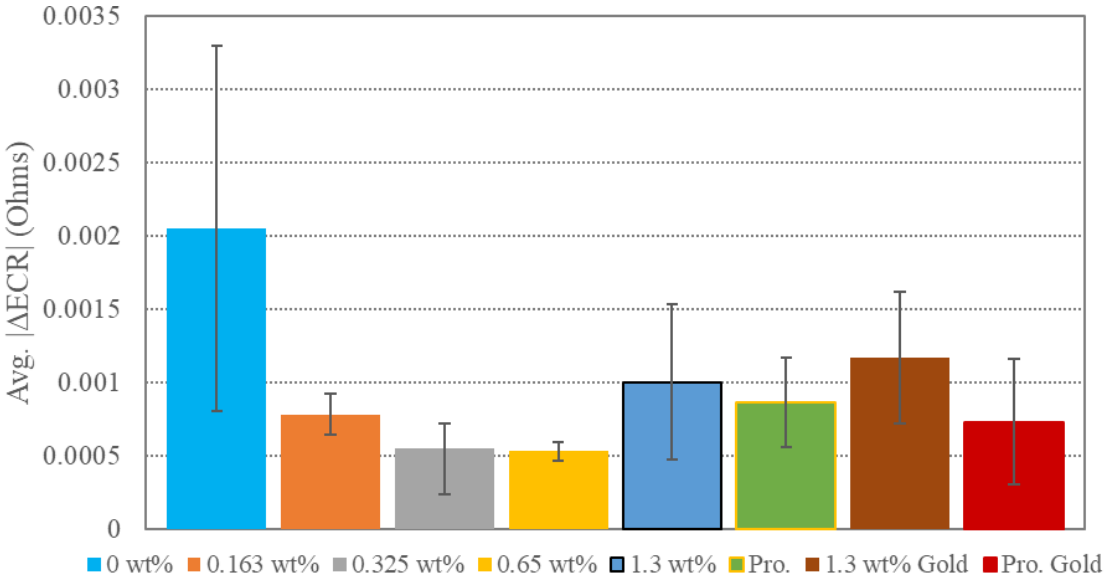

Figure 4.3: Comparison of ECR changes between dodecane nanolubricant and proprietary (Pro.) Stribeck tests; silver sample unless noted otherwise

It can be seen in Fig. 4.3 that adding particles to dodecane results in a lower average ECR change and that there is perhaps a small correlation with the particle concentration, as there are decreases in magnitude until reaching the more uncertain 1.3 wt%. Just as with the friction results (Ch. 3), 0.65 wt% has some of the lowest uncertainty, while 0.325 wt% and 1.3 wt% are 'noisier' and less repeatable. If there was a purely inversely proportional correlation between the particle concentration and change in ECR, then 1.3 wt% should have lower or similar values to 0.65 wt%. There was arguably a slight relative minimum in scar width found for the 0.65 wt% Stribeck tests in Ch. 3, however, and some prior research indicates that wear reduction from particles can have an optimum concentration above which the wear and friction can begin to increase again [8-10, 17]. As will be shown in Ch. 5, the particles reduce adhesion and material transfer while potentially increasing

abrasive friction. Perhaps, then, the balance of these competing mechanisms tips away from reducing changes in ECR past a certain level of abrasive wear and there is an optimum particle concentration around 0.65 wt%.

The proprietary lubricant has similar (& perhaps slightly lower) ECR change to the 1.3 wt% lubricant in Fig. 4.3. The 1.3wt% lubricant on gold samples appears to have slightly higher ECR change, and the proprietary lubricant on gold follows a similar pattern as on silver, being slightly lower than the 1.3 wt% lubricant on gold. This one also has slightly lower ECR change than its silver sample counterpart, unlike the slight increase over silver samples seen with the 1.3 wt% on gold.

Comparing the proprietary lubricant and its related colloids (Fig. 4.4) shows that there is a slight decrease of the average ECR change when adding particles to the proprietary lubricant (the 'proprietary colloid') on silver samples, just as there is when adding particles to the pure dodecane. With gold samples, although the uncertainty is larger, it appears that the proprietary colloid results in higher average ECR changes than the proprietary lubricant. The proprietary solvent colloid (just 'Pro. solvent' in Fig. 4.4, for space) has the lowest levels of ECR change, potentially since there is likely less insulating material around the particles here vs. in a lubricant. Of possible note, the two silver samples which used the proprietary colloid after some of the particles had precipitated out (see Ch. 6) appear to have a slightly lower change in ECR than the ones which had freshly mixed proprietary colloid applied.

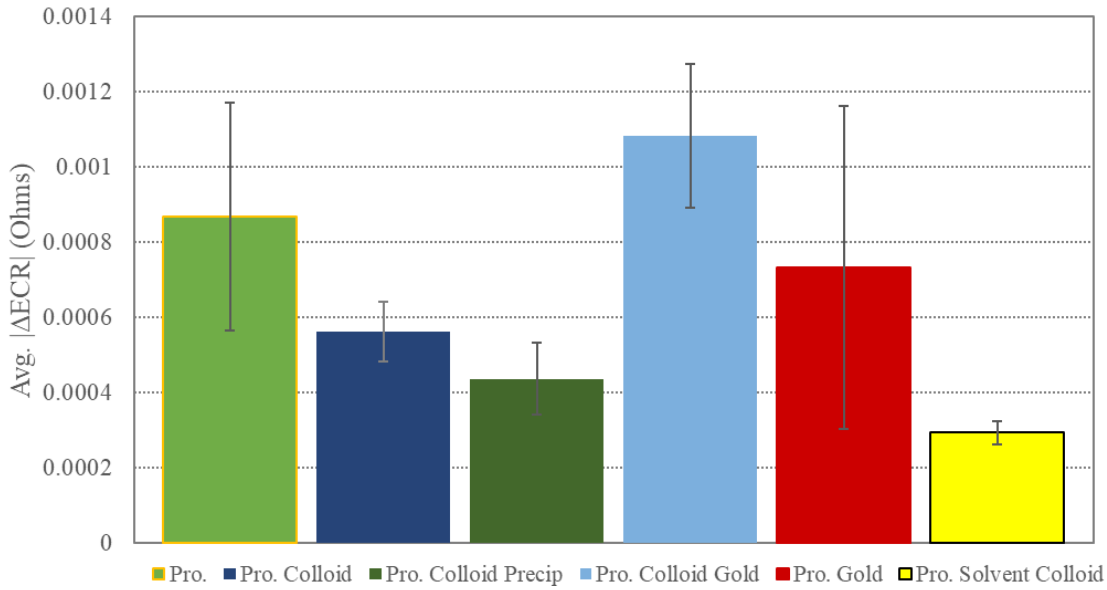

Figure 4.4: Comparison of proprietary (Pro.) lubricant, Pro. Colloid, and Pro. Colloid Solvent for silver/gold Stribeck tests; Also Pro. Colloid after precipitation for limited silver sample Stribeck tests

Next, there is a comparison of the constant speed tests to their Stribeck counterparts (Fig. 4.5). Of note is that the change in ECR is similar between the 1.3 wt% and proprietary lubricants for each test type. Also, an interesting pattern emerged here: the Stribeck test has relatively high ECR change values, followed by a significant drop off when moving to the corresponding 10RPM test, with a significant increase in the 25 RPM test (above the Stribeck test, even). Also interesting is that there is slightly more uncertainty/non-repeatability with the proprietary lubricant than the 1.3 wt% nanolubricant. The uncertainty levels make it difficult to discern if there is a consistent difference between the Stribeck and continuous speed tests here, however, the difference between the 10 and 25 RPM tests appears significant, indicating that there is a consistent difference of some kind between them.

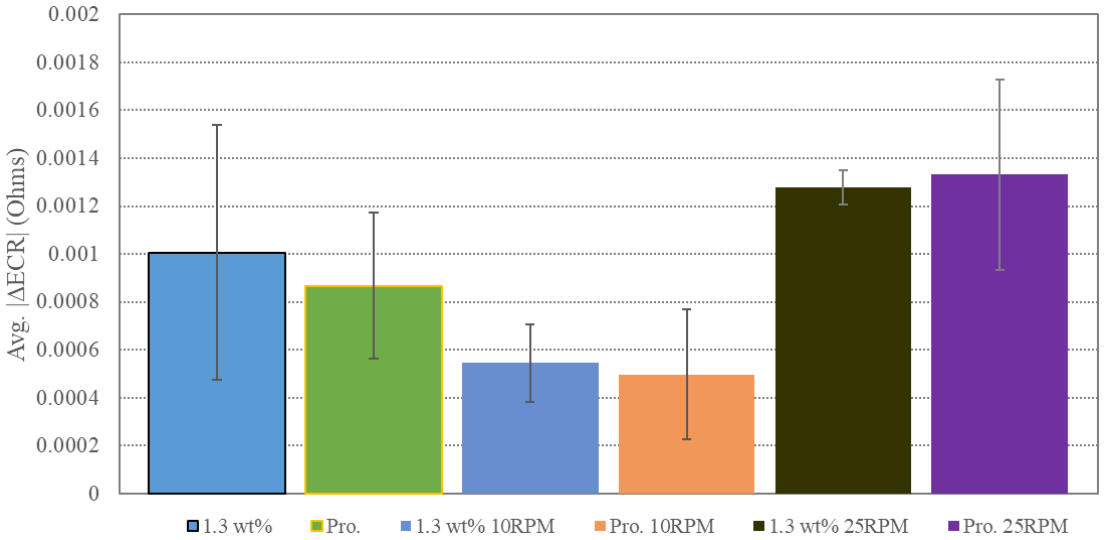

Figure 4.5: Comparison of Stribeck and corresponding continuous speed tests

It is interesting that the 25 RPM tests have larger average changes in ECR than 10 RPM. Not only do the tests cover the same amount of distance for the wear (7770 revolutions), but as will be shown in Ch. 5, the wear on the caps appears slightly worse with the 25 RPM tests (the plates also seem to have more severe wear here, though breakthrough to the nickel barrier appears in only a small streak vs. the entire scar width). This fits with the idea that greater wear and surface changes should result in greater changes to the ECR value.

Finally, there is the comparison of the outlier Stribeck tests and the well-behaved Stribeck tests (Fig. 4.6). The 0.325 wt% outliers seem to have more severe ECR changes, well beyond the error of the well-behaved 0.325 wt% tests. This would fit with the idea that more severe wear (as we see with the outliers in Ch. 5) results in larger average changes to ECR; however, with the 0.163 wt% outliers, the ECR value seems slightly lower. Though the error range casts some doubt on the significance of this difference, it still does not reflect the idea that higher wear => more ECR change. For 0.65 wt%, only one outlier

exists, so calculating standard error is impossible. Regardless, it is similar to the 0.163 wt% outliers in not following the higher wear idea. When combined with the generally high uncertainty/non-reproducibility present in many of the results, it lends credence to the conclusion that multiple factors are at work regarding the change in ECR in these tests.

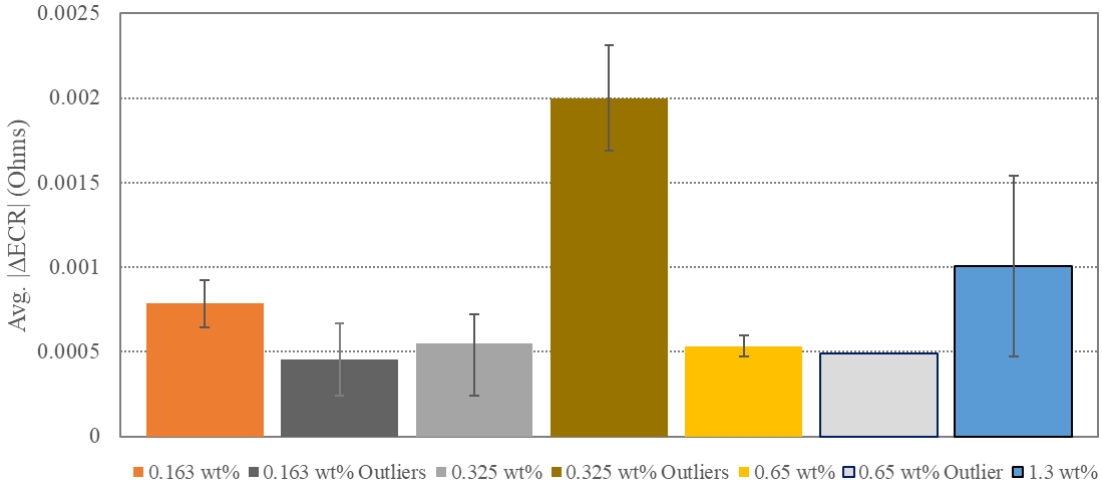

Figure 4.6: Comparison between well-behaved and outlying Stribeck test ECR changes

Ultimately, as these measurements take place with a 2 N loading, the sample surfaces are likely in solid contact; thus, they are more representative of the overall conductivity of the samples in use (prior research has occasionally found very little difference in ECR when applying traditional lubricants, so long as there is only a thin/breakable film present, after all [34]). More specifically, the changes in ECR here are (at least in theory) more likely to be driven by changes to the surface character of the sample plates and caps, rather than a change in conductivity of the lubricant itself. Thus, it is quite interesting that there is not a 100% clear and consistent correlation between wear severity and the average change in ECR.

A potential area for future study is the lubricant conductivity itself, instead of just the effects of the lubricant on/in a contact. This appears to be a somewhat nascent field in the literature and might be useful for electric motor applications (including vehicles); specifically, there is evidence that nanoparticles could enhance the conductivity of a lubricant [21], which could potentially be of use in the prevention of electric discharge-based bearing damage [26]. However, the abrasive wear present with the nanolubricants would present an obstacle to their use within bearings.

Chapter 5–Results: SEM & EDS Analysis of Selected Samples

Given the unusual behavior seen with the nanolubricants (i.e., the outliers, lack of discernable wear scar under stylus profilometry, and decreasing friction at low speeds), SEM and EDS analysis was pursued to clarify what might be driving the results. For this, selected samples were sent to our partners at TE Connectivity for analysis, as detailed in Table 5.1. In general, a 'well-behaved' representative sample was paired with an 'outlier' sample for the dodecane nanolubricants, while a single representative sample was sent for the other included categories.

Table 5.1: Samples sent for SEM/EDS analysis

Name	Particle load (wt%)	Outlier	Test type	RPM	Lubricant
1.3wt % Gold #2	1.3	No	Stribeck	N/A	Dodecane
1.3wt% Silver #1	1.3	No	Stribeck	N/A	Dodecane
0.65wt% Silver #3	0.65	Yes	Stribeck	N/A	Dodecane
0.65wt% silver #7	0.65	No	Stribeck	N/A	Dodecane
0.325wt% Silver #4	0.325	Yes	Stribeck	N/A	Dodecane
0.325wt% Silver #5	0.325	No	Stribeck	N/A	Dodecane
0.163wt% silver #6	0.163	No	Stribeck	N/A	Dodecane
0.163wt% silver #4	0.163	Yes	Stribeck	N/A	Dodecane
0wt% silver #4	0	N/A	Stribeck	N/A	Dodecane
0wt% silver #2	0	N/A	Stribeck	N/A	Dodecane
Pro. Gold #1	N/A	N/A	Stribeck	N/A	Proprietary
Pro. Silver # 3	N/A	N/A	Stribeck	N/A	Proprietary
'Fresh' Pro. colloid Silver #1	~0.65	N/A	Stribeck	N/A	Pro. colloid (fresh)
TE Solvent Silver #1	~1.3	N/A	Stribeck	N/A	Pro. solvent colloid
'Settled' Pro. colloid Silver #2	~0.65	N/A	Stribeck	N/A	Pro. colloid (after settling)
Pro. silver #3 Const.	N/A	N/A	Continuous	10	Proprietary
1.3wt% silver #2 Const.	1.3	N/A	Continuous	10	Dodecane
Pro. silver #1 Const.	N/A	N/A	Continuous	25	Proprietary
1.3wt% silver #2 Const.	1.3	N/A	Continuous	25	Dodecane

Both SEM and EDS analyses were conducted using a Hitachi SU 6600VPSEM with an Oxford EDS detector, using a 20kV accelerating voltage and a working distance of 10-15mm. What follows is a discussion of selected results.

Layered elemental maps from the silver Stribeck tests for 0 wt% dodecane, one of the 0.163 wt% outliers, and the proprietary lubricant are included in Fig. 5.1-5.3. Note that, for the caps (see Ch. 2 for information on the sample sets) used with these lubricants, all appear to feature some amount of material transfer from the plates (Fig. 5.1a-5.3a).

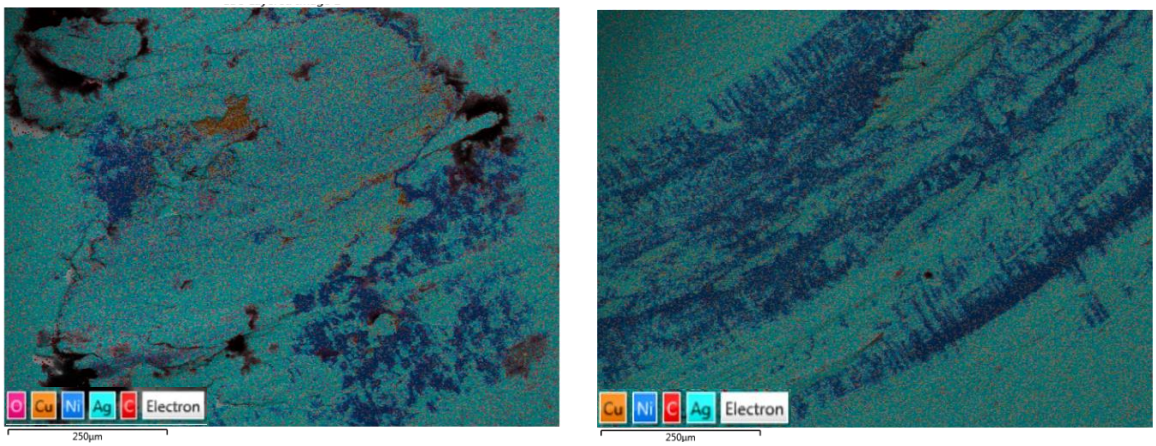

(b) **(a)**

Figure 5.1: Layered elemental map of cap (a) and plate (b) from a 0 wt% Stribeck test

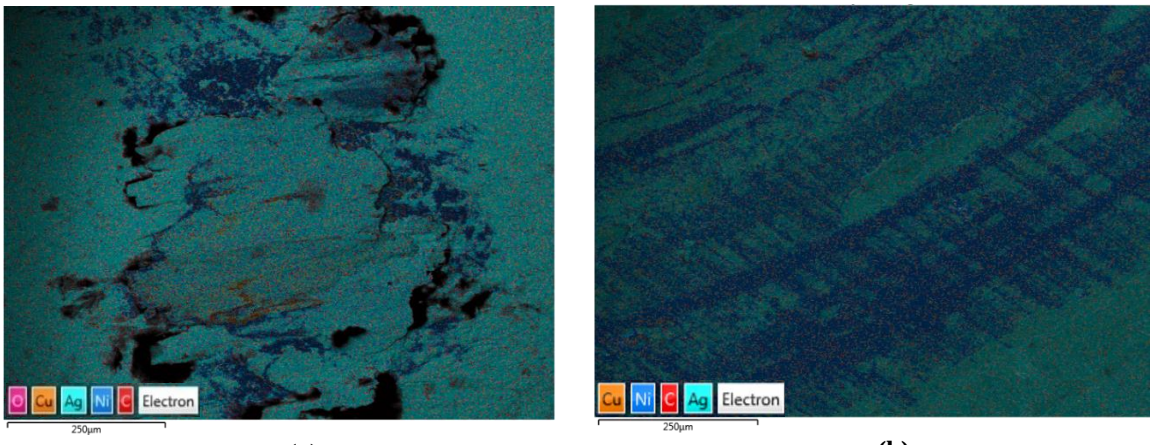

(a) **(b)**

Figure 5.2: Layered elemental map of cap (a) and plate (b) of a 0.163 wt% outlier Stribeck test

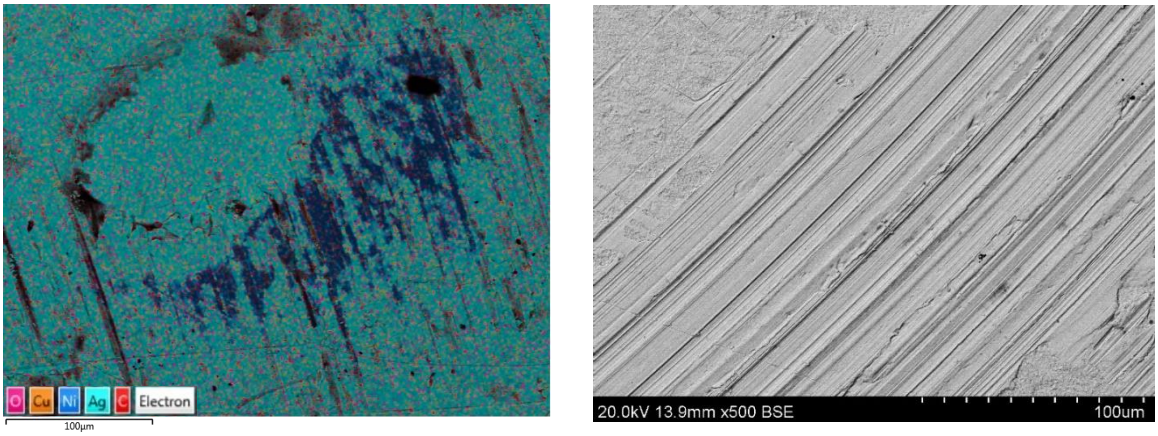

(a) **(b)**

Figure 5.3: Layered elemental map of cap (a) and BSE image of plate (b) of a proprietary lubricant Stribeck test

While the caps all appear to feature material transfer, the size of the scars do vary; the proprietary lubricant scar covers a smaller area (Fig. 5.3a) than the dodecane based lubricants (Fig. 5.1a-5.2a). Additionally, the wear scars of the outliers (0.163 wt% pictured in Fig. 5.2b) and 0 wt% dodecane (Fig. 5.1b) tests feature significant nickel exposure across the wear scar on the plate (this includes the 0.65 wt% and 0.325 wt% outliers, though not explicitly imaged here). Meanwhile, the BSE image of the sample plate from the proprietary lubricant test (Fig. 5.3b) does not show much elemental contrast and it is unlikely that much, if any, exposure of the nickel barrier occurred. This apparent plate-to-cap material transfer represents a common thread among the outlying nanolubricants, proprietary lubricant, and the pure dodecane.

Prior research indicates that the observed material transfer from plate to cap is likely a phenomenon called prow (or wedge) formation, which occurs by adhesive material transfer from the larger material (here, the plate) to the rider (the cap), usually when the rider is continually moved in a single direction over a larger piece of the same material [35]. These are known to be layered and can form cyclically, either by transferring back to

the larger material or by becoming part of the wear debris [35]. While an exact mechanism of formation appears to be unknown, there are some indications that this phenomenon is related to work hardening [36]. Thus, it seems that adhesive wear (and friction as well) is the dominant mechanism present. As will be shown, adhesion appears to dominate without nanoparticles, while abrasion dominates with them, at least for silver samples.

The elemental results are less clear on the gold samples (Fig 5.4-5.5). While the proprietary lubricant Stribeck test seems to have some material changes on the cap (Fig. 5.4a), it is unclear whether this is adhesion/prow formation or another mechanism. The BSE image (Fig. 5.4b) from the plate reveals the porosity of the gold in the wear track and not much else; there is no obvious sign of significant material transfer.

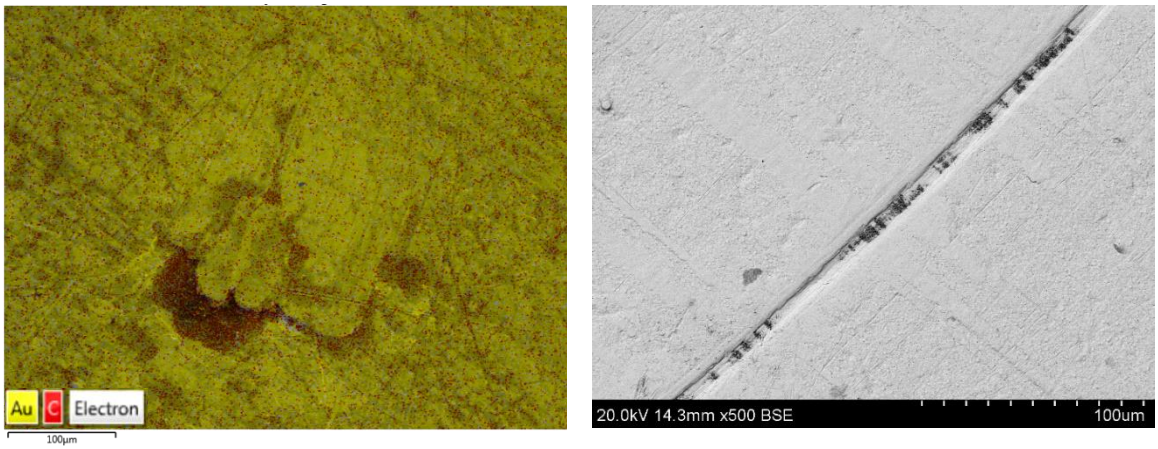

(a) **(b)**

Figure 5.4: Layered elemental map of cap (a) and BSE image of plate (b) of a proprietary lubricant Stribeck test on gold

The 1.3 wt% nanolubricant on gold resulted in the nickel barrier and bronze core bring exposed on the plate (Fig. 5.5b). On the cap, at least the nickel was exposed, though it is unclear if bronze was also exposed (Fig. 5.5a). There appears to be a collection of wear debris on the upper-right side of the cap (as imaged in Fig. 5.5a; though perhaps this is a

prow instead of debris), however the plate scar (Fig. 5.5b) appears free of debris. One notable result is the lack of any silver particles on the plate/cap surfaces, indicating that the particles did not adhere or were only weakly bonded and able to be wiped away by hand cleaning the sample surfaces with acetone/methanol and lint-free wipes. This fits with prior research on silver nanoparticles in polyethylene glycol [15] and indicates that these particles do not create a tribofilm or otherwise 'mend' or modify the surface as has been speculated could be a friction improvement mechanism for nanoparticle lubricants [13, 19].

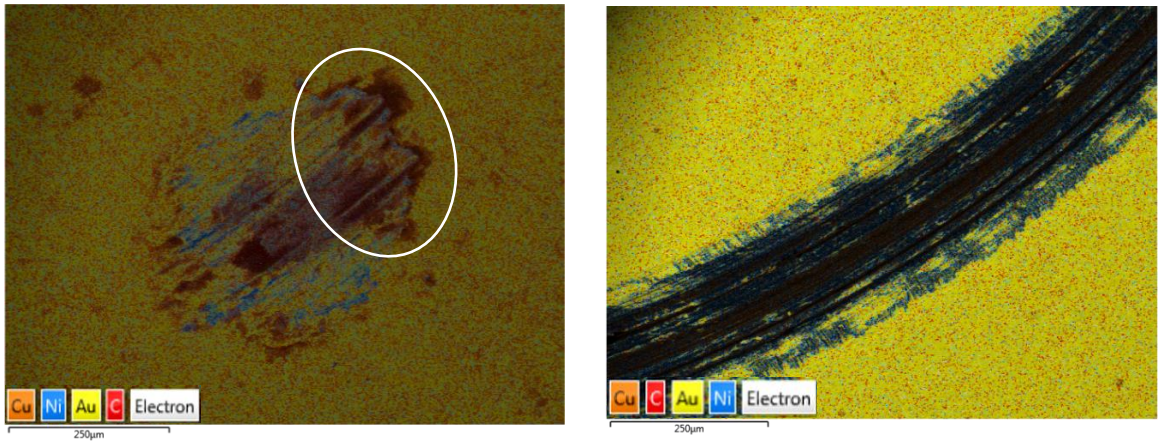

(a) **(b)**

Figure 5.5: Layered elemental map of cap (a) and of plate (b) from a gold 1.3 wt% Stribeck test

All the nanoparticle lubricants on silver samples featured exposure of the nickel barrier on the cap (Fig. 5.6a-5.9a), while the plate either did not have exposure or very little of it (depending on particle concentration). Also notable is the complete lack of a prow/adhesion on the cap for these tests. Representative layered elemental maps of these are shown in Fig. 5.6-5.8.

Note that there is a small amount of nickel barrier exposure within the wear scar (inner edge, or upper left part of Fig. 5.7b) for the 0.163 wt% sample while no such

breakthrough occurs with 1.3 wt% (Fig. 5.6b). This shows that, although the particles are abrasive, having too few particles leads to higher wear during tests, which fits with prior research [8, 10, 11]. Comparing Fig. 5.1-5.3 with the corresponding Fig. 5.6-5.8 reveals that the particles either prevent the transfer of material from the plates to the caps or are abrasive enough to wear away any such transfer (prows) which may occur. Given the lack of nickel exposure on the plates, the former is more likely. The continuous speed tests, discussed shortly, also support this. A notable exception to this lack of prow formation/adhesion, however, is the proprietary solvent colloid where there appears to only be a small amount of material accretion on the cap (Fig. 5.10a). The plate does not feature exposure of the nickel barrier (Fig. 5.10b), though, so it is unclear if it is adhesive material transfer present on the cap.

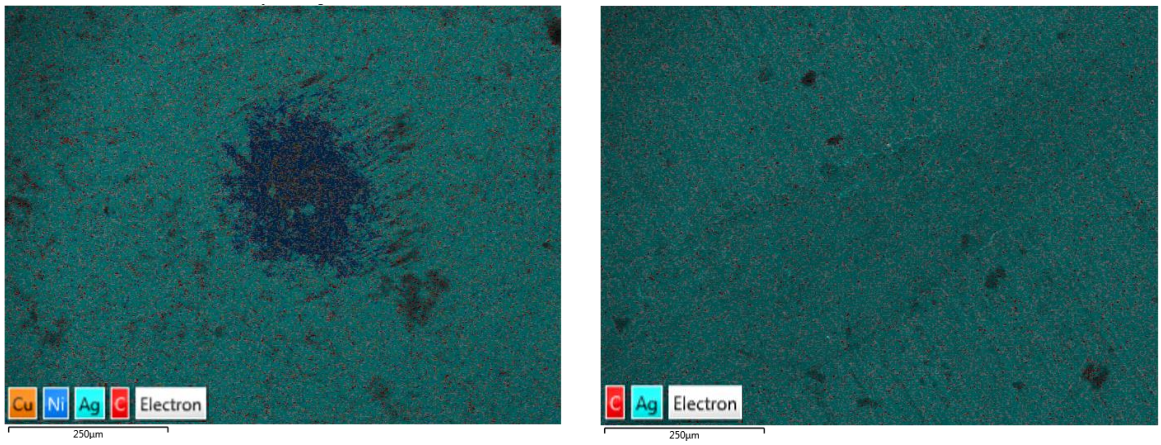

(a) **(b)**

Figure 5.6: Layered elemental map of cap (a) and plate (b) from a 1.3 wt% Stribeck test

Fig. 5.8-5.9 are both from samples used in Stribeck tests performed with the proprietary colloid; however, Fig. 5.9 is from a sample which used proprietary colloid pipetted from the bottom of a container in which it had been allowed to sit so that any reaction/particle precipitation (precipitation discussed in Ch. 2 and 6) could occur. Fig. 5.8

came from a sample tested with freshly mixed proprietary colloid (i.e., it had not been allowed to sit in the container prior to application to the sample plate). The wear on the cap does not appear to be significantly different between the two options (Fig. 5.8a-5.9a), while the plate wear scar has some inconclusive signs of greater adhesive processes being present with the 'settled' proprietary colloid (Fig. 5.9b). It should be noted that a full set of three Stribeck tests was not completed for the settled proprietary colloid (two were performed), as there was no significant difference in friction trend found; this SEM data supports the idea that, although there are stability issues and precipitation, they do not have a significant impact on the friction and wear characteristics vs a proprietary colloid applied immediately after mixing.

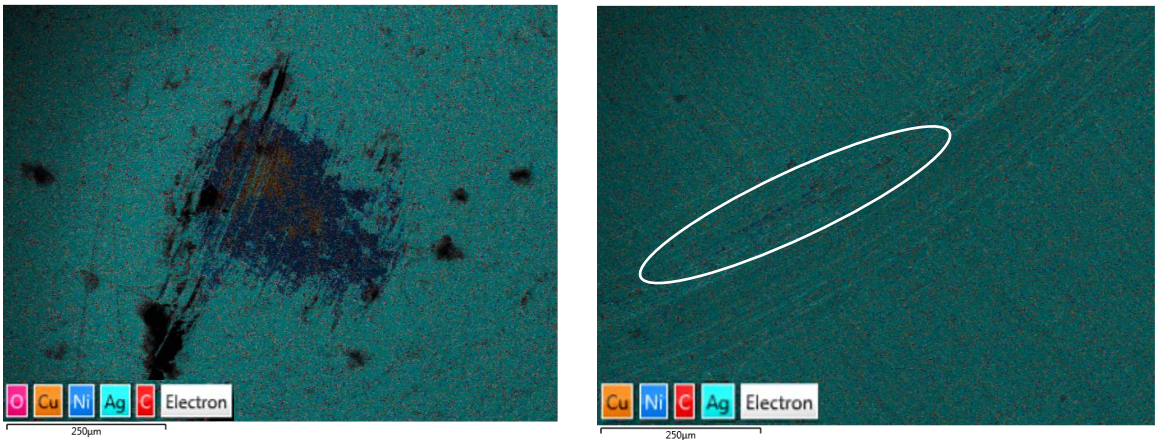

(a) **(b)**

Figure 5.7: Layered elemental map of cap (a) and plate (b) from a 0.163 wt% well-behaved Stribeck test; minor nickel plate exposure in white oval

Fig. 5.11-5.14 are layered element maps taken from representative samples of the continuous speed tests of the 1.3 wt% and proprietary lubricants on silver samples. Comparing the 1.3 wt% and proprietary lubricant samples at 10 RPM (Fig. 5.11 and 5.12, respectively) shows something interesting: the wear on the cap seems slightly deeper/more

severe on the proprietary lubricant sample than 1.3 wt%, though concentrated in grooves (Fig. 5.12a). Additionally, the plates show signs of nickel exposure that is not quite co-located with obvious wear (Fig. 5.11b-5.12b), perhaps a sign that the silver plating was worn thin enough to allow the electrons to penetrate into the underlying nickel barrier a bit while not fully exposing it, or perhaps the result of some cap to plate material transfer.

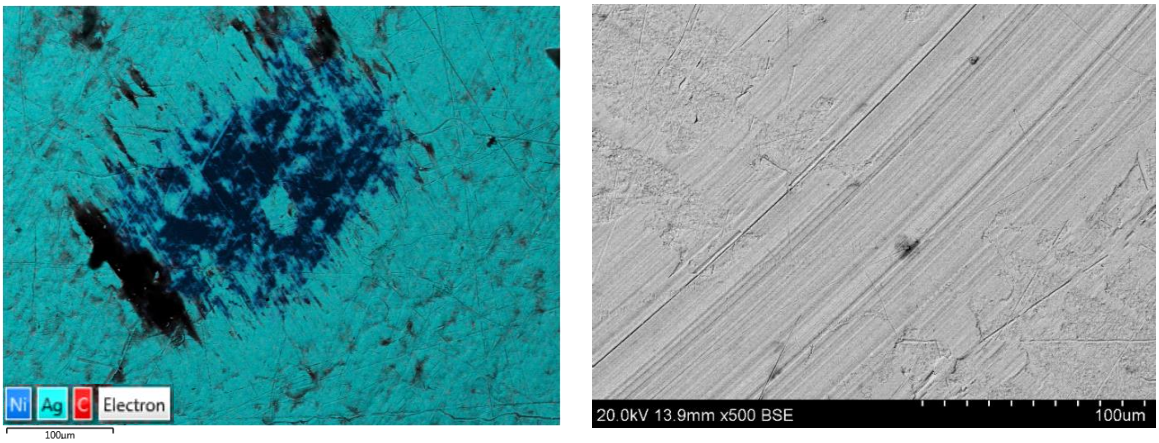

(a) **(b)**

Figure 5.8: Layered elemental map of cap (a) and BSE image of plate (b) from a proprietary colloid Stribeck test

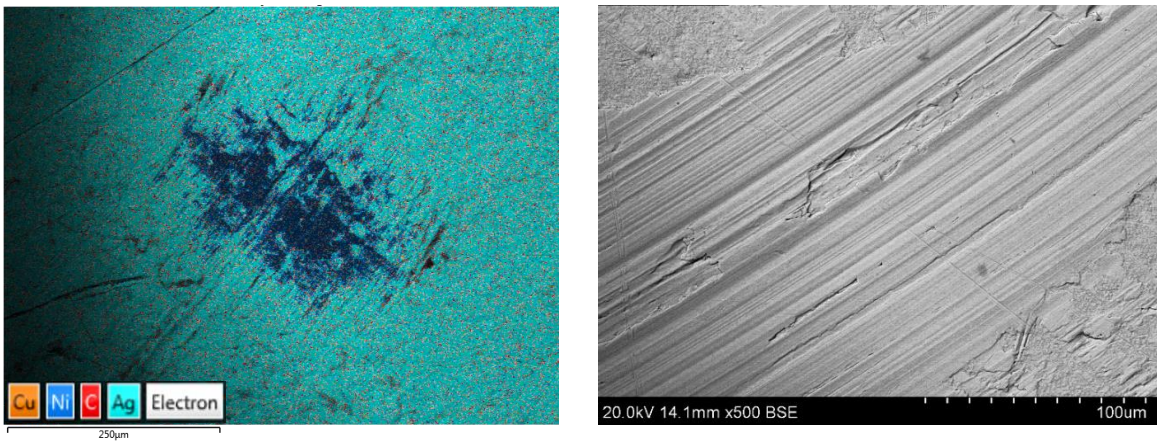

(a) **(b)**

Figure 5.9: Layered elemental map of cap (a) and BSE image of plate (b) from a proprietary colloid (w/settled particles) Stribeck test

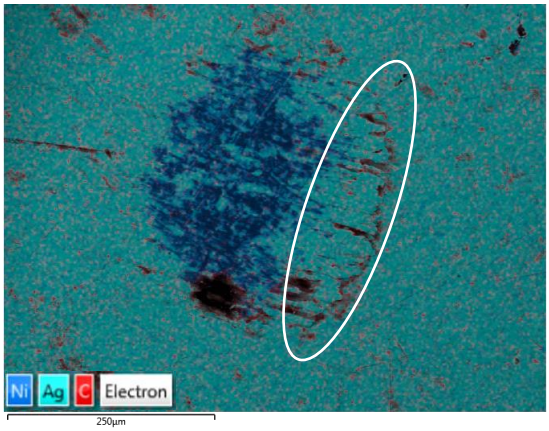

(a)

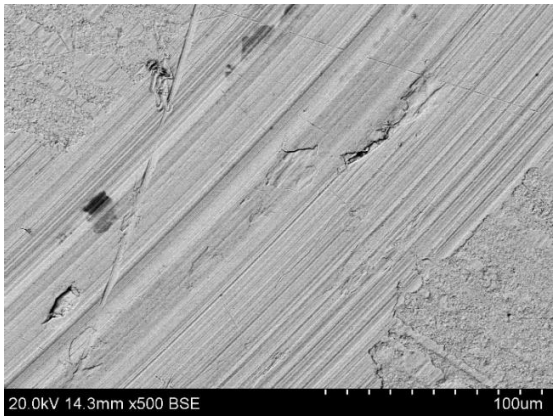

(b)

Figure 5.10: Layered elemental map of cap (a) and BSE image of plate (b) from a proprietary solvent colloid Stribeck test

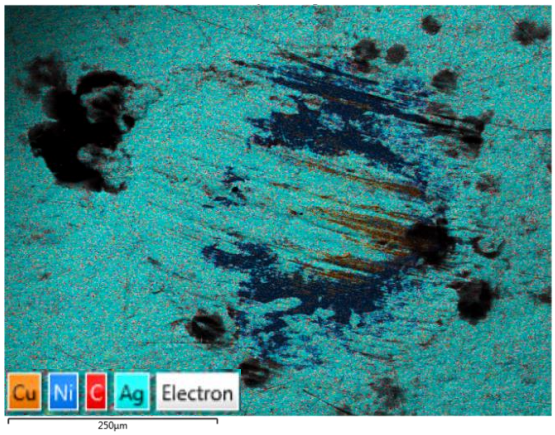

(a)

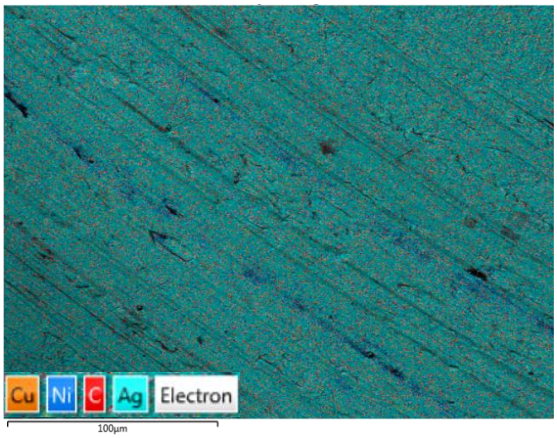

(b)

Figure 5.11: Layered elemental map of cap (a) and plate (b) from a 1.3 wt% 10 RPM continuous test

(a)

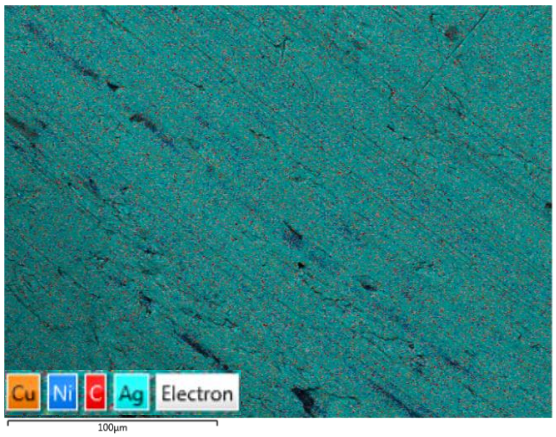

(b)

Figure 5.12: Layered elemental map of cap (a) and plate (b) from a proprietary lubricant 10 RPM continuous test

The wear found for the 25 RPM tests in Fig. 5.13 and 5.14 is more severe than the 10 RPM tests, despite covering the same number of revolutions (and, therefore, distance) in both tests. This makes sense for the nanolubricant, as it did not appear to be in the hydrodynamic regime at these speeds and the recorded friction was higher at 25RPM. However, the proprietary lubricant had lower friction at 25RPM than at 10RPM, making the difference here slightly odd. Notably, the proprietary lubricant featured a larger exposure of nickel on the plate (Fig. 5.14b) than the 1.3 wt% nanolubricant (Fig. 5.13b), despite having less severe wear on the cap (no bronze exposure, Fig. 5.14a) and a lower COF value. For both cases, it appears unlikely that adhesive material transfer from the cap

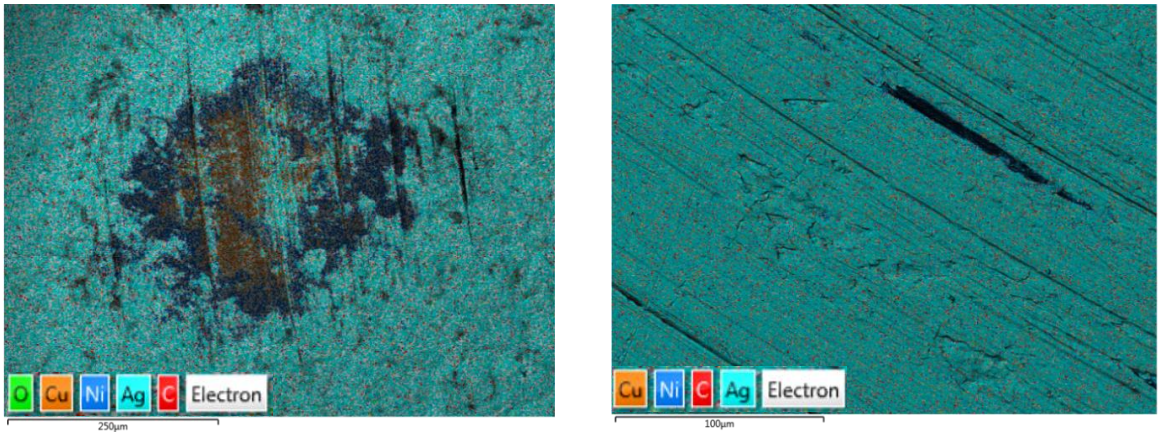

(a) **(b)**

Figure 5.13: Layered elemental map of cap (a) and plate (b) from a 1.3 wt% 25 RPM continuous test

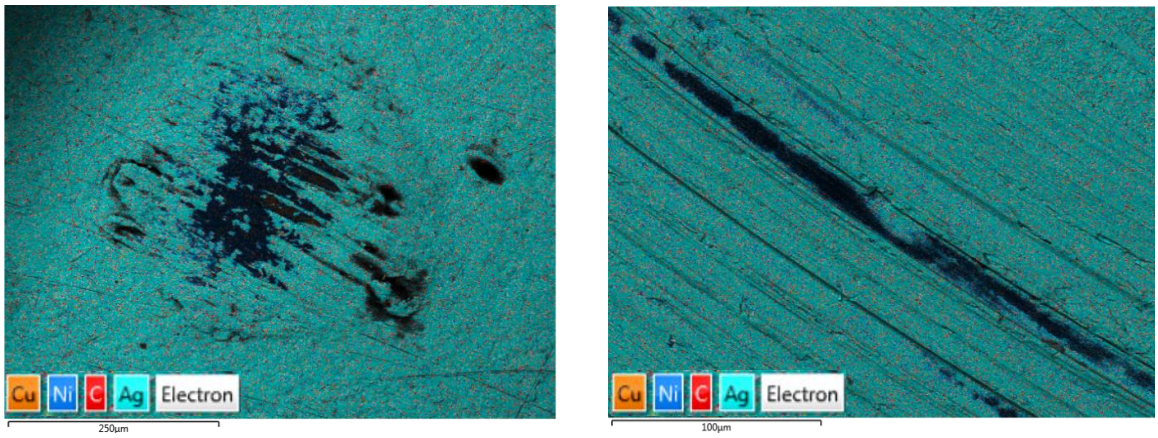

(a) **(b)**

Figure 5.14: Layered elemental map of cap (a) and plate (b) from a proprietary lubricant 25 RPM continuous test

to the plate occurred, lending support to the idea that the 10 RPM plates may have had the silver layer worn thin enough to allow the electrons to penetrate into the underlying nickel barrier layer.

In all the continuous speed tests, no material buildup/prow formation was observed on the cap (Fig. 5.11a-5.14a). While the lack of this with the 1.3 wt% nanolubricant fits with the previously observed trends from the Stribeck tests, the absence of this does not fit with the proprietary lubricant Stribeck tests. This could be an indication that material transfer in the proprietary lubricant Stribeck tests exclusively occurs at higher speeds, then, or perhaps that the proprietary lubricant Stribeck sample analyzed via SEM/EDS is an outlier among its own group. Without further investigation, it is difficult to confirm.

For the 1.3 wt% tests in Fig 5.11 and 5.13, there does not appear to be a consistent signal for what might cause the drop in friction observed during the continuous speed tests (Ch. 3). While both caps feature exposure of the nickel (and bronze, in the 25 RPM test), what looks to be the primary contact area on the 10 RPM cap (Fig. 5.11) is still coated with silver; as there was not a large area of nickel exposure on the corresponding plate (or signs of a central area of higher wear), it is unlikely that this silver was due to significant material transfer from the plate (it also does not appear to be significantly higher than the surrounding material, unlike the previously observed prows on the caps in Fig. 5.1a-5.3a). Instead, it appears that the primary contact area remained silver-on-silver throughout the test. While the 25 RPM test features significant exposure of copper within the primary contact area of the cap, indicating a transition from silver-on-silver to silver-on-nickel to potentially silver-on-bronze sliding, only a single change in friction coefficient was observed during the corresponding test, rather than two (once for silver->nickel, once for

nickel->bronze layer exposures), indicating that the material change was unlikely the singular cause. This supports the hypothesis that polishing/burnishing of the surface (or similar) is another mechanism at work reducing friction with these tests.

Summary

Some key takeaways here include a) adhesion appears to dominate the silver sample Stribeck tests without nanoparticles, while adhesion is eliminated with them (with a possible increase in abrasion). b) the particles do not appear to adhere to the surface in these tests, eliminating mending or film formation as likely friction/wear improvement mechanisms. c) the continuous speed tests do not fall into the same pattern of adhesion vs abrasion present in the Stribeck tests, for unclear reasons. d) in addition to material changes, polishing/burnishing (or similar mechanisms) of the plate surface probably play a role in friction reduction (along with changes from silver-on-silver to silver-on-nickel or perhaps also silver-on-bronze sliding) in the continuous speed tests and perhaps the Stribeck tests as well.

Chapter 6–Results: Lubricant Stability Observations

Throughout the course of running the friction/wear tests, several stability phenomena were observed with the colloids. As mentioned in Ch. 2, these phenomena were explored via leaving lubricant-coated plates in covered culture dishes for extended periods; additionally, the stability of the proprietary-based colloids while inside their mixing containers is discussed. All optical microscope photos were obtained via smartphone camera.

Proprietary Colloid in Containers

The proprietary lubricant is nominally a petroleum-based hydrocarbon with various solid, polymeric, and corrosion preventing components, along with a UV tracer, all suspended in a solvent intended to evaporate after application. After evaporation, a grease-like film (the lubricant) is left on the surface. The full proprietary lubricant (already in solvent) along with the solvent itself were provided to us. Silver nanoparticles were added to the proprietary lubricant via the solvent; that is, the particles were synthesized within the solvent by our colleagues in the Chemistry and Biochemistry department. This proprietary solvent colloid had the same particle concentration of 1.3 wt% as the dodecane and was added to the full proprietary lubricant at a 1:1 volume ratio (e.g., 0.25 mL of proprietary solvent colloid with 0.25 mL of proprietary lubricant). The resulting 'proprietary colloid' should have a particle concentration close to ~0.65 wt%, and it appears to begin precipitating particles within a short amount of time.

Visible precipitation within the proprietary colloids appears to begin within 24-36 hours of colloid mixing (see Fig. 6.1), even when placed in a dark environment immediately after mixing (so, it is not likely a photochemical effect). This is a relatively

slow process, generally finishing within about 7-10 days and is not immediately observable to the eye. The particle precipitation does not appear to completely deplete the particles from the colloid, even once complete, as the liquid portion remains discolored/opaque from the suspended particles (see Fig. 6.2). Additionally, if the developing film is disturbed, the hole will be filled in; however, when the 7–10-day old precipitate film on the bottle surfaces is disturbed, the resulting 'holes' do not become larger/smaller with time (see Fig. 6.3). This indicates that it is possibly the result of the oleyl-sarcosine dropping below the concentration needed to maintain particle stability at the wt% found in the colloid, rather than the lubricant ingredients themselves not reacting well with the particles.

Figure 6.1: Precipitation on sides of bottle after ~36 hrs

Figure 6.2: Precipitation after several days

(a) **(b)**

Figure 6.3: Film disturbances immediately after creation (a) and after 5 days (b); note lack of change

Note that the aforementioned particle precipitation phenomenon was not observed for any of the dodecane colloids (some of which are far more dilute than the proprietary colloid), nor the proprietary solvent colloid (though this seems to have its own type of stability issue). For the dodecane colloids, it appears that they remain shelf stable for several months, at least while stored inside sealed glass containers in a cool/dark location. The proprietary solvent colloid eventually began to show instability signs of a different type, however. Instead of developing a precipitate film like the mixtures in Fig. 3, it started to develop gelatin-esque features (Fig. 6.4) which seem similar to those seen on the 'category 2' sample surfaces (discussed later in this chapter).

Figure 6.4: Proprietary solvent colloid appearing to show deposits after several months of storage

Due to the nature of the container used for the proprietary solvent colloid, it is not possible to verify that the deposits in Fig. 6.4 look like the film features from the category 2 samples under a microscope. Assuming the deposits are the same as the category 2 film features, though, would indicate that they can form without atmospheric exposure, as these formed in the region of the sealed container normally submerged by solvent- not at the

meniscus of it. Regardless, the presence of these effects shows that issues remain with the proprietary lubricant being combined with nanoparticles at this time.

Proprietary Colloid After Application to Plates

Since the proprietary lubricant was designed to have the solvent evaporate before use, all proprietary-based tests allowed for a 24 hr 'drying' period after lubricant application. Once dry, the plates coated with the proprietary colloid generally fell into two categories with roughly equal frequency:

Cat. 1: A consistent/smooth film (see Fig. 6.5a), at least prior to atmospheric exposure

Cat. 2: A rough/dry-looking grease-like surface film (see Fig. 6.6)

All but two category 1 samples exhibited some form of a film 'collapse' shortly after exposure to the atmosphere (see Fig. 6.5b). This collapse generally started within a couple minutes of exposure and took seconds to a few minutes to complete once the start became apparent (although the pictures are of silver samples, this holds true for gold as well) and resulted in a nonuniform film of beaded-up lubricant (perhaps from meniscus stability). This collapse did not appear to make a difference in COF observed.

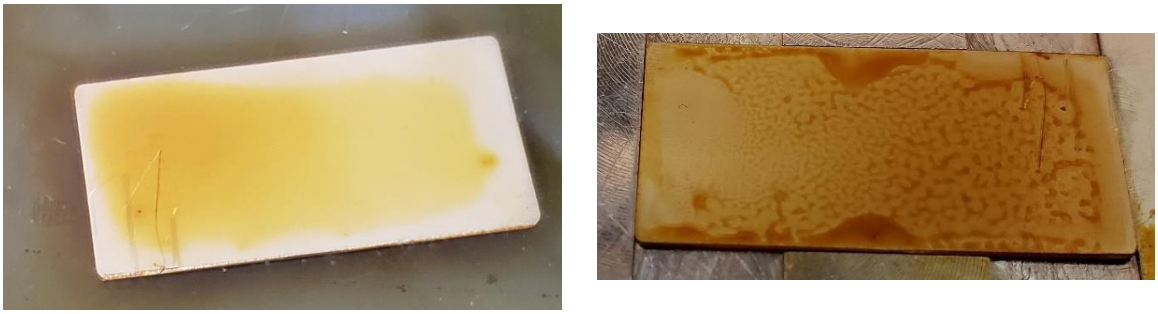

(a) **(b)**

Figure 6.5: Category 1 film (a) and example of film 'collapse' (b)

Figure 6.6: Category 2 example

Category 2 surfaces remained static, without exhibiting a film collapse, after exposure to atmosphere. It is unclear if a category 1 sample that exhibits a film collapse would, after more time passes, become like those in category 2. If so, it would indicate that category 2 surfaces were the result of unobserved film collapses in the covered culture dish and that atmospheric exposure is not necessary to trigger one.

It should be noted that, while film collapse was not observed on samples using the proprietary lubricant, some feature a rough-looking surface reminiscent of those in category 2 (Fig. 6.7a). This is especially apparent when a UV light is used to reveal the tracer (Fig. 6.7b).

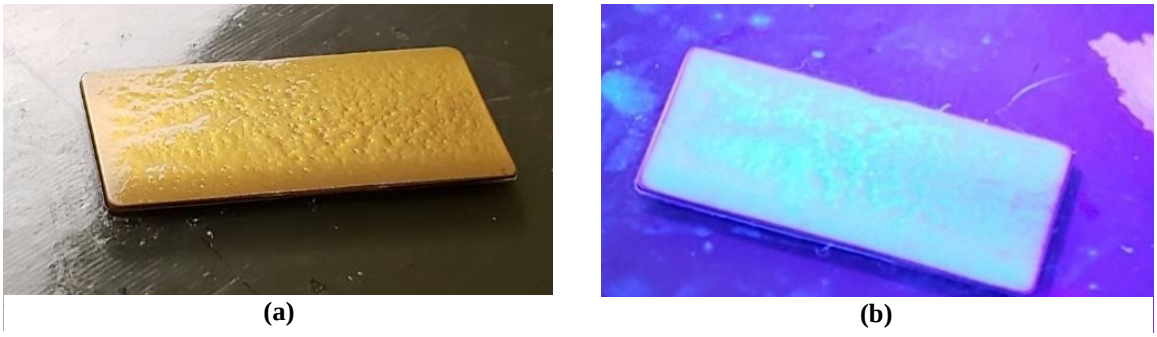

(a) **(b)**

Figure 6.7: Category 2 surface with proprietary lubricant (a) as shown under UV (b) after 24 hours of drying

A category 2 sample was allowed to remain in a covered petri dish for 143 days. To the naked eye, the category 2 surface appeared rough and dry, not changing beyond the initial ~24hr drying time. However, when this sample was observed under the optical microscope, the surface appeared as though it was coated with blobs of some form of gelatin or gel (Fig. 6.8). These gelatin-like deposits present themselves in identical fashion on the gold samples as well (Fig. 6.9), indicating this is not the result of an interaction between the silver surface and silver particles. Given that category 2 samples had similar rough/dry appearing film surface finishes while maintaining low COF and wear during tests (comparable to category 1), it appears that the proprietary colloids are suitable for longer term storage once applied, albeit with a nonuniform film thickness.

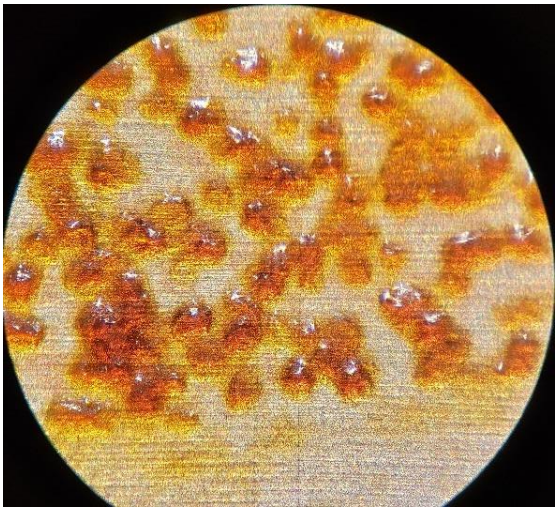

Figure 6.8: Category 2 silver sample under microscope after sitting in covered dish for 143 days

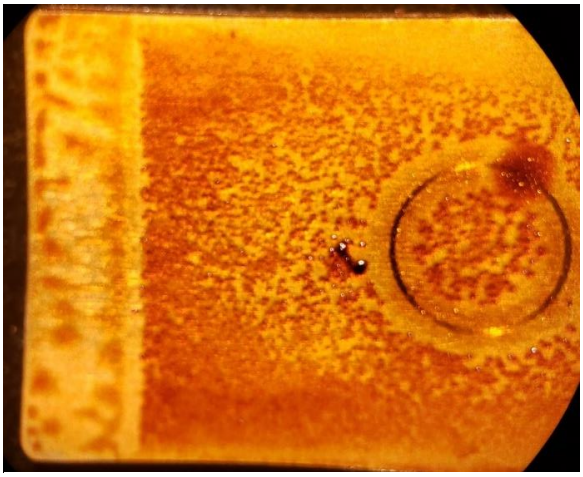

Figure 6.9: Category 2 gold sample under microscope immediately after a stribeck test

Of note, the aforementioned UV tracer is still present in the sample pictured under the microscope in Fig. 6.8. However, the fluorescence only appears in the area which had been accidentally disturbed during handling a couple of months into the test (see Fig. 6.10b). More recent tests showed that fluorescence was completely blocked on gold

samples, even on areas wiped by the pinning bars of the test mounting (see Fig. 6.11a). Silver samples seem to still have some partial fluorescence in areas with film disturbance present (edges and similar, Fig. 6.11b), however.

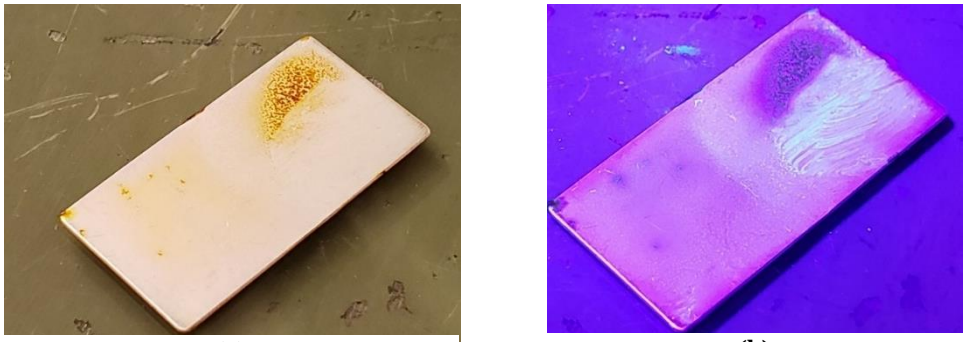

(a) **(b)**

Figure 6.10: Dried sample (a) under UV (b)

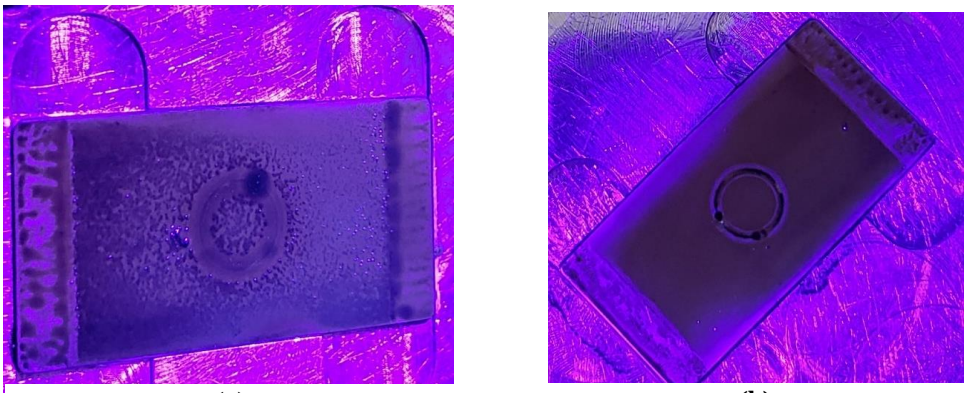

(a) **(b)**

Figure 6.11: UV on gold sample showing complete fluorescence blocking (a); Silver sample showing some fluorescence in disturbed areas (b)

The discrepancy seen in fluorescence results suggests a couple hypotheses:

1. Older film coats are less prone to having particles block UV after being disturbed, perhaps indicating that the particles do not like to move with the film after some time
2. Perhaps this is due to a difference between silver and gold samples with these nanolubricants; i.e., perhaps the silver particles are more difficult to move with the

lubricant when on silver vs the gold, allowing them to be moved ‘out of the way’ of the tracer

Further tests would be required to resolve/confirm this.

Proprietary Solvent Colloid After Surface Application

To explore if the surface film collapses seen with the proprietary colloid (discussed in the preceding subsection) were the result of stand-alone issues with the solvent-particle mix or something which only occurred with the proprietary colloid, the proprietary solvent colloid was applied directly to two fresh silver sample plates and allowed to undergo the typical 24hr drying period in a covered culture dish. The resulting films did not fit either category or exhibit film collapses. As can be seen in Fig. 6.12a, the film was not consistent, yet it was relatively smooth overall. A brief exploration under a microscope (Fig. 6.12b) showed some signs of localized film thickening, as in the category 2 surfaces, however these areas did not resemble a gelatin like the category 2 surfaces (this thickening instead has more in common with the features of the dodecane drying tests discussed in the next subsection).

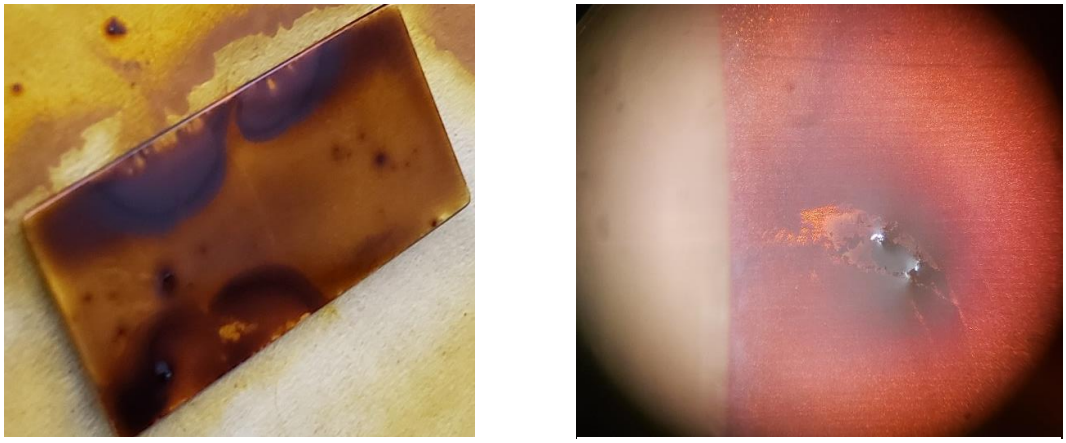

(a) **(b)**

Figure 6.12: Proprietary solvent colloid on surface after 24 hrs (a); film 'peak' under microscope (b)

Dodecane Nanolubricant After Application to Plates

The drying behavior of the dodecane nanolubricants was explored to see if there were any similarities to the proprietary colloids. Two fresh silver sample plates were coated with the 1.3 wt% dodecane nanolubricant and left in separate covered culture dishes for 132 days (with an initial check after 24 hours of drying). An interesting progression was observed. Initially, silver plates coated with the dodecane nanolubricants have their entire surfaces tinted brown. However, after 24hrs, the surfaces were generally coated in a clear film interspersed with 'dots' (Fig. 6.13a), which were probably related to locally enhanced particle concentrations. After 38 days (Fig. 6.13b), the surface had become completely tinted again (perhaps as a result of wicking the lubricant surrounding the plate after 24hrs back onto the plate surface), while maintaining the 'dots' in the same locations seen after 24hrs. Beyond this point, minimal changes (if any) were observed, even after 132 days (see Fig. 6.14).

(a) **(b)**

Figure 6.13: 1.3 wt% dodecane after 24 hrs (a) and 38 days (b)

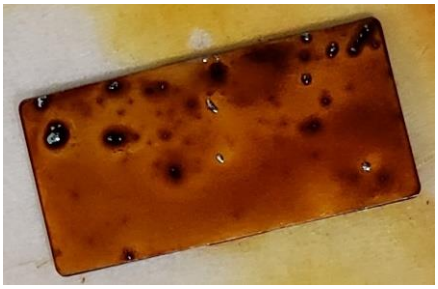

Figure 6.14: 1.3 wt% dodecane after 132 days

The ‘dots’ seen on the silver plates after a long period of sitting appear to be areas of thicker film and possibly a higher concentration of nanoparticles. When viewed under the optical microscope (Fig. 6.15), the surfaces appear to be coated in many randomly distributed small and ‘flat’ ‘dots’ under the film/tinting (Fig. 6.15a), with the larger ‘dots’ appearing to be areas of thicker film (Fig. 6.15b).

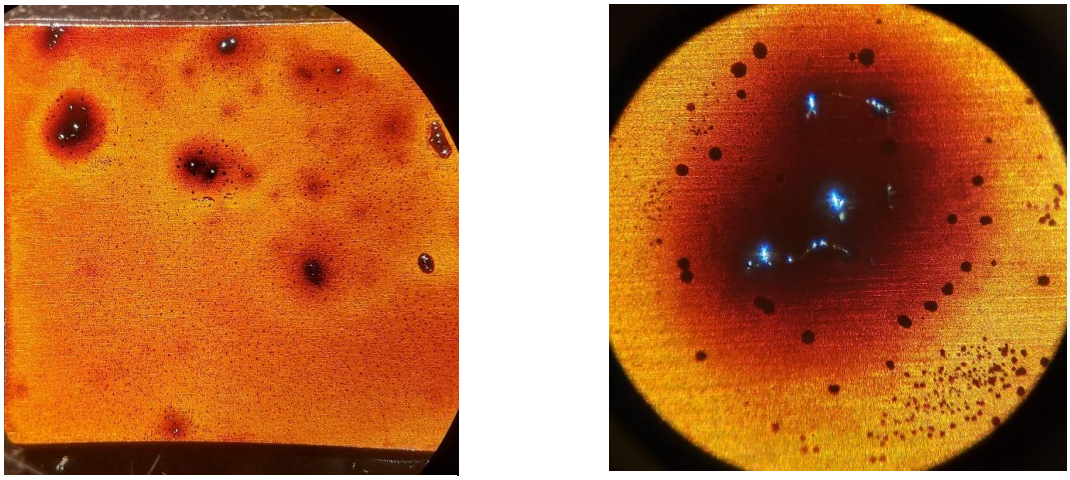

(a) **(b)**

Figure 6.15: Microscope images of the 1.3 wt% silver plate samples after 132 days (a), closeup (b)

The thicker film areas do not appear to correlate with areas of particularly concentrated ‘flat’ ‘dots’ and it is difficult to ascertain what might cause these features; although, since they are randomly scattered, there is likely some role played by the microscale surface features (and perhaps also surface tension and/or meniscus formation) here. It does appear that some form of local film thickening is often present in all the colloids once dried, although it is present in the most extreme form within the proprietary colloids. Of note is that, often, areas of samples left in contact with a surface retained a more liquid film; this could indicate that these lubricants would be most useful within connectors that are usually in contact, with small times of separation.

Chapter 7–Results: Film Thickness Calculation

The Bruker ECR readings did not indicate that the experiments reached the full-film lubrication regime (i.e., ECR did not indicate that the surfaces were out of contact) for either the dodecane or proprietary lubricants. At most, as based on the proprietary lubricant Stribeck curves, it seems the EHL regime could have been reached. To explore this with the dodecane lubricants, calculations of the approximate minimum and central film thicknesses were made and are detailed here.

Several assumptions were made for the calculations to follow, including, e.g., that the pin and plate samples were made of a single material instead of being multi-layer/plated objects and that the flooded hard-EHL equations would fit the situation. Additionally, the viscosity values obtained/used were for pure dodecane, not the nanoparticle version. It is known from prior work that nanoparticles can increase the viscosity of a lubricant [8]. However, even increasing the viscosity by the average of 20.4% found in that paper (an overestimate for the 1.3 wt% dodecane nanolubricant, as this was a 2 wt% nanoparticle loading) does not produce a significant increase in the film thicknesses. The Hamrock & Dowson hard-EHL flooded elliptical contact equations were used as follows [37, 38]:

$$\bar{h}_{min} = R_x * 3.63\left(\frac{\eta_o \bar{u}}{E' R_x}\right)^{0.68} * (\alpha E')^{0.49} * \left(\frac{force}{E' R_x^2}\right)^{-0.073} * \left(1 - \exp\left(-0.68 * \left(\frac{R_y}{R_x}\right)^{\frac{2}{\pi}}\right)\right) \quad (1)$$

$$\bar{h}_c = R_x * 2.69\left(\frac{\eta_o \bar{u}}{E' R_x}\right)^{0.67} * (\alpha E')^{0.53} * \left(\frac{force}{E' R_x^2}\right)^{-0.067} * \left(1 - 0.61 * \exp\left(-0.73 * \left(\frac{R_y}{R_x}\right)^{\frac{2}{\pi}}\right)\right) \quad (2)$$

$$Where\ R_x = R_y = R = equivalent\ radius;\ E' = Equivalent\ modulus;\ \eta_0 = viscosity$$

$$\alpha = Barus\ Pressure - Viscosity\ coefficient; \bar{u} = \frac{linear\ speed}{2} = mean\ velocity;$$

The radius of curvature of the cap was calculated using data from a white light interferometer measurement of a bronze (unplated) cap sample (see Fig. 7.1). Since the cap samples are hemispheres, only one radius, R, was calculated as R_x and R_y for (1) and (2) were equal. All relevant material properties (for silver and gold) were obtained via Matweb and are shown in Table 7.1 [39, 40]. To calculate the radius of curvature, it was assumed that the measured curve accurately represented the arc of the circle which would be formed from extending the hemisphere. The radius was calculated from (3) [41].

$$R = \frac{W^2}{8H} + \frac{H}{2}; (3)$$

Where $W = base\ width\ of\ arc; H = height\ from\ base\ to\ peak\ of\ arc$

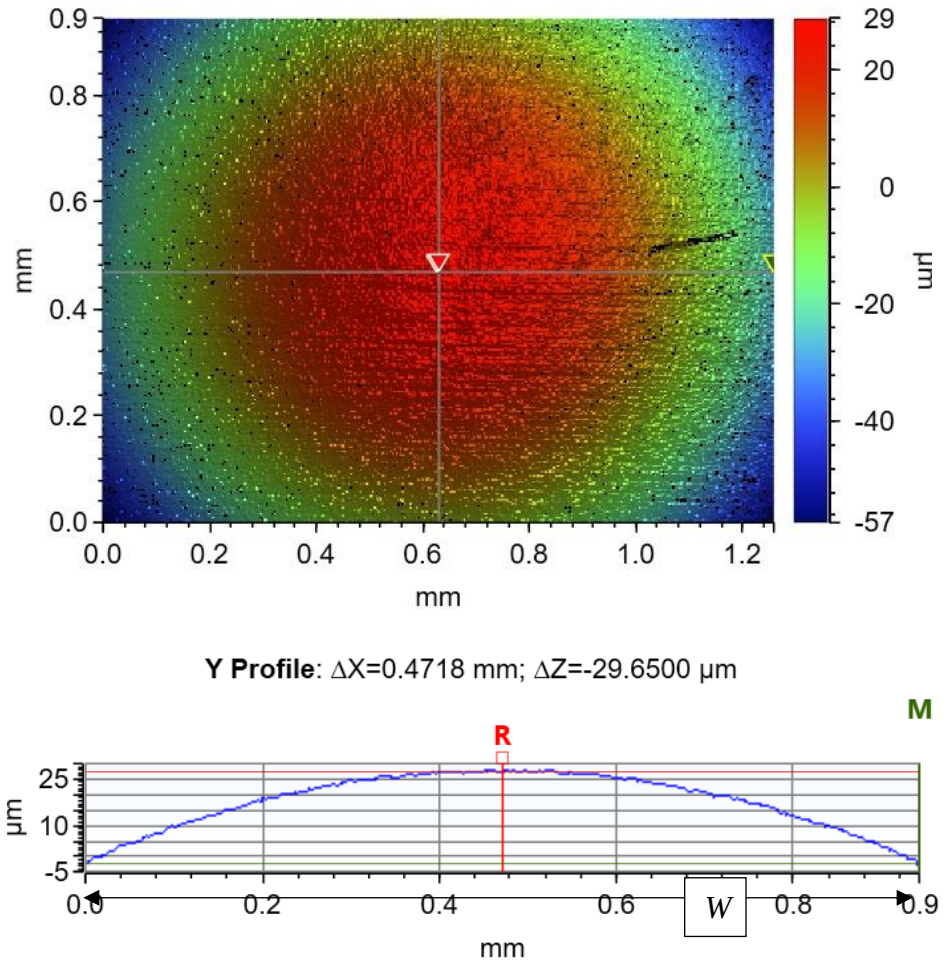

Figure 7.1: Interferometer data, including the y-direction slice used for radius (R) calculation

For the radius of curvature (R) calculation, the width (W) and height (H) of the arc were directly taken from the data shown in Fig. 7.1 above:

W = 0.9mm; H = Δz = 29.65μm

$$R = \frac{0.9mm^2}{8(29.65\mu m)} + \frac{29.65\mu m}{2} = 3.43mm$$

Since the pin rests on a flat plate, the equivalent radius became the following:

$$R_x = R_y = R = 3.43\ mm$$

Since the pin and flat are the same material, the equivalent modulus calculation was as follows (sample calculation given for silver):

$$E' = \frac{E}{(1-\upsilon^2)} = \frac{76}{(1-0.37^2)} = 88.1GPa$$

Table 7.1: Silver and Gold Material Properties Used

Material	E (GPa)	Poisson's Ratio, υ	E' (GPa)
Silver	76	0.37	88.1
Gold	77.2	0.42	93.7

A table of pressure-correlated viscosity data was obtained for pure dodecane [42]. The room-temperature (298.25K) values from this were used with an exponential fit to obtain the Barus Pressure-Viscosity coefficient, as shown in Fig. 7.2. The equation was set to fit the initial viscosity at zero pressure.

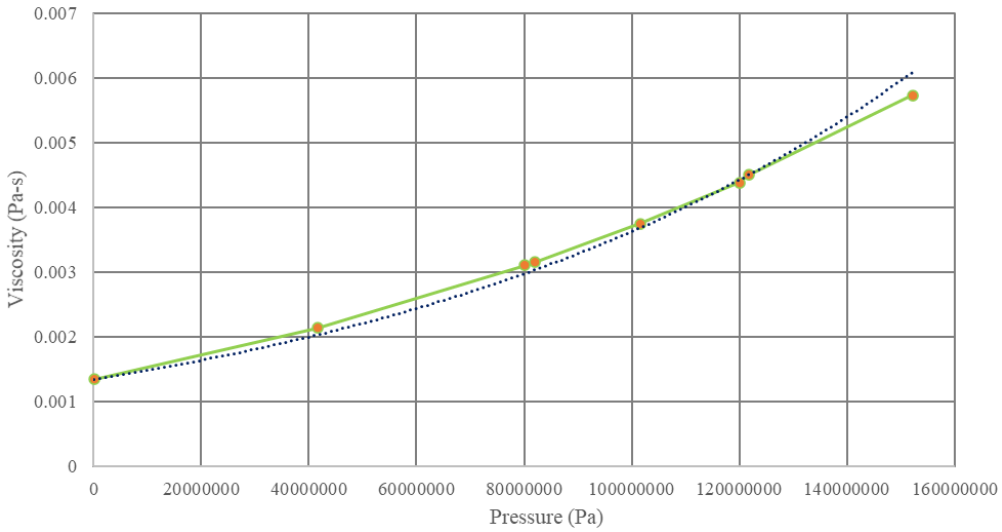

Figure 7.2: Viscosity vs. Pressure used to obtain Barus coefficient via exponential fit (black dotted line)

The exponential curve fit in Fig. 7.2 yielded the following viscosity and Barus pressure-viscosity coefficient/eq:

$$\eta = 1.344mPa - s * e^{9.92722\frac{1}{nPa}} \quad (4)$$

$$\eta_0 = 1.344mPa - s;\ \alpha = 9.92722\frac{1}{nPa}$$

The mean velocity used in (1) and (2) was calculated from the top speed of 0.163 m/s (resulting in $\bar{u} = 0.0815$ m/s), with a force of 2 N, as taken from the experimental procedures (Ch. 2). Using these parameters with (1), (2), and (4) in a simple MATLAB script (see Appendix B for code) yielded the approximate film thicknesses, as detailed in Table 7.2.

Table 7.2: Film Thickness Calculation Results

Material	Minimum thickness (nm)	Central thickness (nm)	Surface Roughness (R_a)
Silver	1.54	2.63	0.95-1.07 µm
Gold	1.53	2.62	0.34-0.35 µm

Both film thicknesses are far smaller than the TE-provided average surface roughness values (R_a) for silver of 0.95-1.07 μm, further confirming that the full-film regime is not reached at even the top speeds tested. For gold, the TE-provided surface roughness values were 0.34-0.35 μm, again far higher than the film thickness. These results indicate that the full-film regime was not reached with dodecane or dodecane nanolubricants at any point during the Stribeck tests.

Chapter 8: Conclusion

An exploration of the effects of adding silver nanoparticles to both dodecane and a proprietary lubricant was performed. Varying speed tests from 0.163 m/s to 0.001 m/s were performed to generate Stribeck curves and explore the lubrication regimes present. These tests also featured measurements of the ECR changes and the severity of the wear scars.

Stribeck tests showed that nanoparticles had markedly lower friction coefficients and narrower/less severe wear scars than seen with pure dodecane, even closing in on the lower friction performance of the proprietary lubricant when at speeds lower than 25 RPM (0.007 m/s) when using the highest tested particle concentration of 1.3 wt%. Additionally, continuous speed tests showed that the abnormal reduction of COF at low speed with the dodecane nanolubricants on silver plated samples was not likely to be purely the result of wear effects exposing the nickel, with plate surface polishing/burnishing potentially playing a role, along with some indications that the silver nanolubricant itself had a role.

Adding particles to the proprietary lubricant (to get the 'proprietary colloid') appears to have had little impact on the friction levels for the silver samples, with COF levels being similar across the speeds tested (though it was slightly lower between 100 RPM/0.027 m/s and 200 RPM/0.054 m/s), while slightly wider wear scars were generated. However, for gold samples, the COF at speeds below 50 RPM (0.014 m/s) dramatically increased when using the proprietary colloid, perhaps because of gold thin-film lubrication effects as the gold plating got worn down [28]. The exact mechanism causing the trend is unclear, however. The 1.3 wt% dodecane nanolubricant produced severe wear on the gold samples, completely exposing the nickel barrier layer and part of the bronze core, marking it as relatively unusable with a gold surface. On the silver samples with the dodecane

nanolubricant dilutions, wear scar severity followed the results from prior research in being near-inversely proportional to the concentration of nanoparticles, particularly when viewed through SEM.

ECR changes across the tests proved difficult to measure. From an analysis of just the average magnitude (not direction) of the changes across tests, there seems to be a weak inverse correlation between nanoparticle concentration and change in ECR, with increases at 1.3 wt% indicating there could be an optimum concentration around 0.65 wt%. However, the particles do improve average ECR change magnitude over the pure dodecane, bringing it to a level competitive with the proprietary lubricant and, at least for the 0.65 wt% level, potentially giving it a slight advantage over the proprietary lubricant on silver samples.

SEM and EDS analysis of the silver samples confirmed that particle concentration is inversely related to the level of wear on the plate and revealed adhesive material transfer to the caps as a common feature between the pure dodecane, outlying nanolubricant tests, and possibly the proprietary lubricant. It remains unclear if this is true adhesive material transfer for the proprietary lubricant as well since the plate in that case did not feature nickel exposure. This material transfer was also missing from the proprietary lubricant constant speed tests. Adhesive material transfer was not present in any of the well-behaved nanolubricant Stribeck tests, indicating that adhesive friction/wear dominate without particles while the particles effectively eliminate it and potentially increase the abrasion. On the gold samples, no silver nanoparticle transfer was observed to the surfaces, implying that mending or the generation of a tribofilm is unlikely to be a method of friction reduction for these silver nanoparticles.

The dodecane nanolubricants (including dilutions) appear stable for at least 1 year, 11 months (and counting), though there might be some photosensitivity; as such, they should be kept away from light to keep stable. After application, the dodecane appears to 'dry out' on the surfaces and leave behind locally thick areas of film which are potentially areas of relatively enhanced nanoparticle concentration. If the surface is in contact with something else, the lubricant appears to not dry out for an extended period.

Synthesizing silver nanoparticles in the evaporative solvent for the proprietary lubricant results in a very stable colloid, although after several months some signs of instability have become apparent. As with the dodecane, some signs of photosensitivity suggest storage in a dark place. Mixing this colloid with the full proprietary lubricant results in an initially unstable 'proprietary colloid' which precipitates over the course of about a week before reaching an equilibrium; past this point, no more particles will precipitate out of the solution. However, this instability, along with observed plate film nonuniformities, do not appear to markedly affect the friction/wear performance of the proprietary colloid during tests and could be the result of the stabilizer (oleyl-sarcosine) being diluted out. More investigation would be required to confirm this.

For dodecane based lubricants, it is likely that tests remained in the boundary regime, as seen in the Stribeck curves and the approximate EHL film thickness calculations. Though the proprietary lubricant curves imply that full film was reached, the Bruker ECR measurements did not indicate a complete lack of contact.

Overall, adding silver nanoparticles to the dodecane improved the friction/wear/ECR performance to a similar level as the proprietary lubricant, indicating that these particles have potential electrical contact uses and should be explored further.

References

1. Zhang, Jie, and Hugh Spikes. "On the mechanism of ZDDP antiwear film formation." *Tribology Letters* 63, no. 2 (2016): 1-15.
2. Jackson, Robert L., Alex B. Coker, Zoe Tucker, Mohammad Sharif Hossain, and German Mills. "An Investigation of Silver-Nanoparticle-Laden Lubricants for Electrical Contacts." *IEEE Transactions on Components, Packaging and Manufacturing Technology* 9, no. 2 (2018): 193-200.
3. Greer, Julia R., and William D. Nix. "Size dependence of mechanical properties of gold at the sub-micron scale." *Applied Physics A* 80, no. 8 (2005): 1625-1629.
4. Gerberich, W. W., J. Michler, W. M. Mook, R. Ghisleni, F. Östlund, D. D. Stauffer, and R. Ballarini. "Scale effects for strength, ductility, and toughness in “brittle” materials." *Journal of Materials Research* 24, no. 3 (2009): 898-906.
5. Choi, S. US, and Jeffrey A. Eastman. *Enhancing thermal conductivity of fluids with nanoparticles*. No. ANL/MSD/CP-84938; CONF-951135-29. Argonne National Lab., IL (United States), 1995.
6. Darvin, Jason R., Mohammad Sharif Hossain, Mahdi Nabil, Jamie Uertz, and G. Mills. "Concentrated Ag Nanoparticles in Dodecane as Phase Change Materials for Thermal Energy Storage." *ACS Applied Nano Materials* 2, no. 10 (2019): 6187-6196.
7. Pordanjani, Ahmad Hajatzadeh, Saeed Aghakhani, Masoud Afrand, Boshra Mahmoudi, Omid Mahian, and Somchai Wongwises. "An updated review on application of nanofluids in heat exchangers for saving energy." *Energy Conversion and Management* 198 (2019): 111886.

8. Ghaednia, Hamed, Robert L. Jackson, and Jeyhoon M. Khodadadi. "Experimental analysis of stable CuO nanoparticle enhanced lubricants." *Journal of Experimental Nanoscience* 10, no. 1 (2015): 1-18.

9. Gu, Cai-xiang, Guan-jun Zhu, Lei Li, Xiao-yu Tian, and Guang-yao Zhu. "Tribological effects of oxide based nanoparticles in lubricating oils." *Journal of Marine Science and Application* 8, no. 1 (2009): 71-76.

10. Gara, Luan, and Qian Zou. "Friction and wear characteristics of oil-based ZnO nanofluids." *Tribology Transactions* 56, no. 2 (2013): 236-244.

11. Gara, Luan, and Qian Zou. "Friction and wear characteristics of water-based ZnO and Al2O3 nanofluids." *Tribology Transactions* 55, no. 3 (2012): 345-350.

12. Novak, Caymen, David Kingman, Kyle Stern, Qian Zou, and Luan Gara. "Tribological properties of paraffinic oil with nanodiamond particles." *Tribology Transactions* 57, no. 5 (2014): 831-837.

13. Liu, Gang, X. Li, B. Qin, D. Xing, Y. Guo, and R. Fan. "Investigation of the mending effect and mechanism of copper nano-particles on a tribologically stressed surface." *Tribology Letters* 17, no. 4 (2004): 961-966.

14. Shenderova, O., A. Vargas, S. Turner, D. M. Ivanov, and M. G. Ivanov. "Nanodiamond-based nanolubricants: investigation of friction surfaces." *Tribology Transactions* 57, no. 6 (2014): 1051-1057.

15. Ghaednia, Hamed, M. Sharif Hossain, and Robert L. Jackson. "Tribological performance of silver nanoparticle–enhanced polyethylene glycol lubricants." *Tribology Transactions* 59, no. 4 (2016): 585-592.

16. Tao, Xu, Zhao Jiazheng, and Xu Kang. "The ball-bearing effect of diamond nanoparticles as an oil additive." *Journal of Physics D: Applied Physics* 29, no. 11 (1996): 2932.

17. Ghaednia, Hamed, and Robert L. Jackson. "The role of nanoparticles in lubricants; performing lubricated and dry friction tests." *Tribol. Lubric. Technol* 71, no. 7 (2015): 20-24..

18. Zhang, M., et al., *Performance and anti-wear mechanism of Cu nanoparticles as lubricating oil additives.* Industrial Lubrication and Tribology, 2009. **61**(6): p. 311-318.

19. Lee, Kwangho, Yujin Hwang, Seongir Cheong, Youngmin Choi, Laeun Kwon, Jaekeun Lee, and Soo Hyung Kim. "Understanding the role of nanoparticles in nano-oil lubrication." *Tribology Letters* 35, no. 2 (2009): 127-131.

20. Ghaednia, Hamed, and Robert L. Jackson. "The effect of nanoparticles on the real area of contact, friction, and wear." *Journal of Tribology* 135, no. 4 (2013).

21. Minea, Alina Adriana. "A review on electrical conductivity of nanoparticle-enhanced fluids." *Nanomaterials* 9, no. 11 (2019): 1592.

22. Campbell, W. "The lubrication of electrical contacts." *IEEE Transactions on Components, Hybrids, and Manufacturing Technology* 1, no. 1 (1978): 4-16.

23. Chen, Y., S. Jha, A. Raut, W. Zhang, and H. Liang. "Performance Characteristics of Lubricants in Electric and Hybrid Vehicles: A Review of Current and Future Needs. Front." *Mech. Eng* 6 (2020): 571464.

24. Willwerth, Adam, and Matthew Roman. "Electrical bearing damage—a lurking problem in inverter-driven traction motors." In *2013 IEEE Transportation Electrification Conference and Expo (ITEC)*, pp. 1-4. IEEE, 2013.

25. He, Feng, Guoxin Xie, and Jianbin Luo. "Electrical bearing failures in electric vehicles." *Friction* 8, no. 1 (2020): 4-28.

26. Suzumura, Junichi. "Prevention of electrical pitting on rolling bearings by electrically conductive grease." *Quarterly Report of RTRI* 57, no. 1 (2016): 42-47.

27. *File:Stribeck curve.svg*. 2021; Available from: https://commons.wikimedia.org/wiki/File:Stribeck_curve.svg.

28. Antler, M., and T. Spalvins. "Lubrication with thin gold films." *Gold bulletin* 21, no. 2 (1988): 59-68.

29. Ludema, Kenneth C., and Layo Ajayi. *Friction, wear, lubrication: a textbook in tribology*. (CRC press, 2018), 111

30. Brockman, IRVIN H., C. S. Sieber, and R. S. Mroczkowski. "A limited study of the effects of contact normal force, contact geometry, and wipe distance on the contact resistance of gold-plated contacts." *IEEE Transactions on Components, Hybrids, and Manufacturing Technology* 11, no. 4 (1988): 393-400.

31. Van Dijk, Piet. "Critical aspects of electrical connector contacts." *Proc. 21st ICEC* (2002): 161-168.

32. Slade, Paul G., ed. *Electrical contacts: principles and applications*. (CRC press, 2017), 427

33. “Adjusting NPLC and Aperture to make high speed measurements.” *Keysight.* 2021; Available from:

https://www.keysight.com/main/editorial.jspx%3Fcc%3DUS%26lc%3Deng%26ckey%3D710001-1-eng%26nid%3D-33254.0.00%26id%3D710001-1-eng?&cc=US&lc=eng

34. van Dijk, Piet. "Some effects of lubricants and corrosion inhibitors on electrical contacts." *AMP Journal of Technology* 2 (1992): 56-62.

35. Cocks, M. "Interaction of sliding metal surfaces." *Journal of Applied Physics* 33, no. 7 (1962): 2152-2161.

36. Antler, Morton. "Metal transfer and the wedge forming mechanism." *Journal of Applied Physics* 34, no. 2 (1963): 438-439.

37. Hamrock, Bernard J., and Duncan Dowson. "Isothermal elastohydrodynamic lubrication of point contacts: part III—fully flooded results." (1977): 264-275.

38. Hamrock, Bernard J., Bernard J. Schmid, and Bo O. Jacobson. *Fundamentals of fluid film lubrication*. (Vol. 169. CRC press, 2004), 490-499

39. *Silver, Ag*. 2021; Available from: http://www.matweb.com/search/DataSheet.aspx?MatGUID=63cbd043a31f4f739ddb7632c1443d33.

40. *Gold, Au*. 2021; Available from: http://www.matweb.com/search/datasheet.aspx?matguid=d2a2119a08904a0fa706e9408cddb88e&ckck=1.

41. *Radius of an Arc or Arch with calculator - Math Open Reference*. 2011; Available from: https://www.mathopenref.com/arcradius.html.

42. Caudwell, D. R., J. P. M. Trusler, V. Vesovic, and W. A. Wakeham. "The viscosity and density of n-dodecane and n-octadecane at pressures up to 200 MPa and temperatures up to 473 K." *International Journal of Thermophysics* 25, no. 5 (2004): 1339-1352.

Appendix A: MATLAB Script for Breaking Apart/analyzing Bruker .csv Files

```
% Some basic analysis stuff


clear all
close all
clc

[filename, pathname] = uigetfile({'*.*'},'Pick an excel file');
fullname = fullfile(pathname, filename);
test = readmatrix(fullname);

%test = xlsread('Stribeck_feb_02_20_065wtwet_025ml_newdmm_silver5.xlsx');
stepcount = length(rmmissing(test(:,1)));
steps = 1:stepcount;

t = rmmissing(test(:,11));
ECR = rmmissing(test(:,4));
COF = rmmissing(test(:,13));
rpm = rmmissing(abs(test(:,9)));
Fx = rmmissing(abs(test(:,1)));
Fz = rmmissing(abs(test(:,2)));



zero_loc = zerofinder(t); %get the splitting locations
[tvec,tve] = vecslice(zero_loc,t); % split the vector of interest;
ECR_vec = vecslice(zero_loc,ECR);
COF_vec = vecslice(zero_loc,COF);
rpm_vec = vecslice(zero_loc,rpm);
Fx_vec = vecslice(zero_loc,Fx);
Fz_vec = vecslice(zero_loc,Fz);
my_cof_vec = Fx_vec./Fz_vec;
tvec_mins = tvec./60;

for i = 1:length(zero_loc)
    figure(i)
    plot(tvec(:,i),COF_vec(:,i))
%     plot(tvec(:,i),ECR_vec(:,i))
%     plot(tvec(:,i),rpm_vec(:,i))
end


time = adjcat(zero_loc,tve);
time_mins = time./60;

my_cof = Fx./Fz;

function locs = zerofinder(T)

    stepcount = length(T);

    k = 1;
    loc = 1;
    for i = 1:stepcount-1
        T(i);
        if T(i+1) == 0

            loc(k+1) = i+1;
            k = k + 1;
        else
        end
    end
    locs = loc;
end
```

```
% slice the vectors into each step since time resets to 0 at each step
function [tvec,tve] = vecslice(locs,T)

for i = 1:length(locs)

    if i < length(locs)
        loc = locs(i);
        loc2 = locs(i+1);
    else
        loc2 = length(T);
        loc = locs(i);
    end
    m = 1;
%     tve = {1};
    for k = loc:loc2-1
        Tvec(m) = T(k);
        m = m + 1;
    end
    tve(i,:) = {Tvec};
    Tvec = 0;
    m = 1;
end

if 13 == length(tve)
    tvec = padcat(tve{1,1}',tve{2,1}',tve{3,1});
else
    tvec = padcat(tve{1,1}',tve{2,1}',tve{3,1}');
end

end


function tvec = adjcat(locs,T)
% to make the time vector into a single, ever increasing sequence
    timesum(1) = 0;
    temptime = T{1,:};

    for i = 2:length(locs)
        timesum(i) = timesum(i-1) + temptime(length(temptime));
        temptime = T{i,:};
    end
    tee = T{1,:};
    for k = 2:length(locs)
        temptime = T{k,:};

        for i = 1:length(temptime)
            loc = locs(k);
            tee(loc+(i-1)) = timesum(k) + temptime(i);
        end
    end
    tee((locs(length(locs))+length(T{3,:}))) = NaN;
    tvec = tee;
end
```

Appendix B: MATLAB Script for Film Thickness Calculations

```
% because it's easier than using the calculator over and over
clc
clear all

% Silver stuff
%E_p = 88.1e9; nu = 0.37; % poisson's ratio

% Gold stuff
E_p = 93.7e9; nu = 0.42; % poisson's ratio

% fluid stuff
visc = 1.34e-3; % Pa-s
%visc = 1.61e-3; % Pa-s, with 20.4 % increase
R = (3.43e-3); % m
vel = 0.163/2; % m/s
%alpha = 7.9/1e9; % 1/Pa % from those charts, more approximate?
alpha = 0.00000000992722; % from exponential fit
w = 2; % N
ratio = 1; % since ball-on-plate test is very similar

% Central Thickness
h_c =
R*(2.69*(((vel*visc)/(E_p*R))^0.67)*((alpha*E_p)^0.53)*((w/(E_p*(R^2)))
^-.067)*(1-0.61*exp(-0.73*(ratio^(2/pi)))))
% Minimum Thickness
h_min =
R*(3.63*(((vel*visc)/(E_p*R))^0.68)*((alpha*E_p)^0.49)*((w/(E_p*(R^2)))
^-.073)*(1-exp(-0.68*(ratio^(2/pi)))))
```